International Journal of Hydrogen Energy 234 (2026) 154957

Contents lists available at ScienceDirect

International Journal of Hydrogen Energy

journal homepage: www.elsevier.com/locate/he

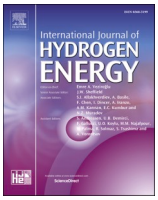

Environmental Potential Of Co-Transporting Hydrogen In Natural Gas Pipelines Followed By Electrochemical Hydrogen Compression

Karan Anand [a], Georgia Ioanna Prokopou [b], Wibke Zängler [c], Vu Phong Nguyen [d], Hendrik Pötting [a], Robert Keller [c], Alexander Mitsos [b,e,f], Matthias Wessling [c,g], Niklas von der Assen [a,*]

[a] RWTH Aachen University, Institute of Technical Thermodynamics, Schinkelstr. 8, 52062, Aachen, Germany
[b] RWTH Aachen University, Process Systems Engineering, Forckenbeckstr. 51, 52074, Aachen, Germany
[c] RWTH Aachen University, Chemical Process Engineering, Forckenbeckstr. 51, 52074, Aachen, Germany
[d] TLK Energy GmbH, Heinrichsallee 41, 52062, Aachen, Germany
[e] JARA-ENERGY, 52056, Aachen, Germany
[f] Institute of Climate and Energy Systems, Energy Systems Engineering (ICE-1), Forschungszentrum Jülich GmbH, 52425, Jülich, Germany
[g] DWI - Leibniz Institute for Interactive Materials, RWTH Aachen University, 52074, Aachen, Germany

ARTICLE INFO

Keywords:
Electrochemical hydrogen compression
Hydrogen separation
Hydrogen supply chain
Life cycle assessment
Hydrogen and natural gas co-transport

ABSTRACT

Green hydrogen (H_2) produced via water electrolysis and renewable electricity is promising to defossilize energy-intensive sectors. Options to deliver H_2 to consumers include H_2 pipelines as well as co-transport in existing natural gas (NG) pipelines. H_2/NG co-transport requires subsequent separation and compression, as H_2 consumers require high-purity H_2 at elevated pressures. Electrochemical Hydrogen Compression (EHC) is an emerging technology for both separation and compression. We conduct a cradle-to-gate Life Cycle Assessment of H_2/NG co-transport in NG pipelines with EHC. We compare H_2/NG co-transport with EHC against co-transport with Pressure Swing Adsorption, pure H_2 pipelines, and fossil H_2, among others, with respect to 16 environmental impact categories. H_2/NG co-transport with EHC can achieve similar greenhouse gas (GHG) emissions as pure H_2 pipelines, and can reduce GHG emissions by up to 91% compared to fossil H_2 if the supply chain is powered by wind electricity. However, if the GWI of electricity exceeds ~260 $g_{CO2\text{-}eq}/kWh_{el}$, all green H_2 transport routes have higher GHG emissions than fossil H_2. Furthermore, these GHG emission reductions are accompanied by increased environmental impacts in at least 9 categories.

1. Introduction

The mitigation of climate change requires the defossilization of energy-intensive sectors, such as chemicals, steel and mobility. In many cases, direct electrification using renewable electricity sources (RES) is a viable option [1,2]. However, direct electrification poses challenges for some energy-intensive sectors because they require energy carriers with high gravimetric energy densities [3]. One promising energy carrier is green hydrogen (H_2), produced via water electrolysis and renewable electricity [4]. Since green H_2 is often not produced where it is consumed, an infrastructure is needed to transport H_2 [5]. One of the main challenges for storage and transport is hydrogen's low volumetric density [6].

Pipelines are considered a promising H_2 transport option due to low emissions compared to other options [7]. The infrastructure for pipelines exists in many countries for transport of natural gas (NG) [8], e.g., 500,000 km in Germany [9,10]. The existing NG pipeline infrastructure can be retrofitted to either co-transport H_2 with NG, or to transport H_2 in dedicated pure H_2 pipelines [11,12]. Consequently, both pure H_2 pipelines and co-transport in NG pipelines are part of H_2 distribution strategies of some countries, such as Australia [13] and Germany [9,10].

Co-transporting H_2 in NG pipelines requires subsequent separation and compression of H_2 since most H_2 consumers, e.g., H_2 refueling stations, require high-purity H_2 at elevated pressures [14,15]. Pressure Swing Adsorption (PSA) is a well-established technology for H_2 separation from high-concentration feeds in industrial processes such as Steam Methane Reforming (SMR) [16]. However, PSA has not been used for separating H_2 from feeds with relatively low concentrations of H_2,

* Corresponding author.
E-mail address: niklas.vonderassen@ltt.rwth-aachen.de (N. von der Assen).

https://doi.org/10.1016/j.ijhydene.2026.154957
Received 16 January 2026; Received in revised form 13 March 2026; Accepted 8 April 2026
Available online 21 April 2026

such as up to 20 vol.-% in H_2/NG co-transport [16–20]. Furthermore, additional mechanical compressors are needed in PSA systems, which can be energy-intensive [17]. A promising emerging alternative is Electrochemical Hydrogen Compression (EHC), which can both separate and compress H_2 in a single device [18,21]. Theoretically, EHC has the potential to achieve purities greater than 99.97 % [18] at up to 900 bar [22] with H_2 recovery rates up to 100 % [20]. Currently, practical challenges such as high energy demands up to 16 kWh/kg_{H2} [15] due to high ohmic losses and back-diffusion of H_2 lower the overall performance of EHC [20,23].

For H_2/NG co-transport including subsequent separation and compression via EHC to be a viable transport option, its economic feasibility and environmental impacts should be favorable over those of H_2/NG co-transport with PSA as well as alternative pure H_2 transport routes. While economic feasibility drives technology adoption, green H_2 is deployed to meet environmental sustainability targets, and therefore the environmental impacts of H_2/NG co-transport with EHC need to be comparable to or lower than those of alternative H_2 supply routes. However, these environmental impacts have not been comprehensively assessed, making it unclear whether H_2/NG co-transport with EHC can enable H_2 supply at low environmental impacts.

Neacsa et al. [24] calculated the Global Warming Impact (GWI) of combusting H_2/NG mixtures, while Cappello et al. [25] and Di Lullo et al. [26] determined the GWI during transport and combustion of H_2/NG mixtures. Davis et al. [27] assessed the GWI mitigation potential and cost effectiveness of H_2/NG mixtures across an economy. Bellocchi et al. [28] determined the environmental impacts of H_2/NG mixtures across multiple scenarios, while considering blended end-use. None of the mentioned studies considered the subsequent separation and compression of H_2 from NG and in particular, none assessed EHC as an alternative separation and compression technology from an environmental perspective. Further, the mentioned studies did not compare the environmental impacts of H_2 supply via NG pipelines to other H_2 transport routes. Aminov et al. [29] compared H_2/NG co-transport to other H_2 transport routes from an economic perspective while considering membranes for H_2 separation. Di Lullo et al. [30] compared the greenhouse gas (GHG) emissions of H_2/NG co-transport to other H_2 transport routes while considering PSA for H_2 separation. The study demonstrated that the lowest costs and GHG emissions are achieved through H_2/NG co-transport and pure H_2 pipelines [30].

In summary, studies assessing the environmental impacts of H_2/NG co-transport remain limited. In particular, no study determined the environmental impacts of H_2 separation and compression via EHC. Thus, the environmental potential of H_2/NG co-transport with subsequent separation and compression via EHC, as well as its comparison to alternative H_2 supply routes, remains an open research gap.

Our study closes the identified research gaps by conducting a cradle-to-gate Life Cycle Assessment (LCA) of H_2 separation and compression via EHC, as well as H_2/NG co-transport in NG pipelines with EHC to enable H_2 supply. For H_2 separation, we include PSA as alternative technology in our assessment. We further compare the environmental impacts of H_2/NG co-transport to other promising H_2 transport options, i.e., transport in new pure H_2 pipelines, transport of liquid H_2 in fuel-cell electric trucks, and the transport of electricity with H_2 production at consumer-site. Fossil H_2 from SMR serves as benchmark. We also assess the risk of environmental burden-shift by evaluating 16 environmental impact categories, as recommended by the Joint Research Center (JRC) of the European Commission [31]. Furthermore, we perform in-depth parameter variations covering various pipeline assumptions, mixture conditions, transport distances and GHG emissions for the electricity used in the supply chain to obtain potential environmental trade-offs with other H_2 transport options. Ultimately, the aim of this study is to assess the environmental potential of supplying H_2 through the existing NG infrastructure using EHC.

2. Life Cycle Assessment (LCA)

The environmental assessment is conducted through an LCA as defined in the ISO 14040/44 standards [32]. An LCA study is conducted in four steps: 1) Goal and scope definition, 2) Life Cycle Inventory (LCI), 3) Life Cycle Impact Assessment (LCIA) and 4) Interpretation [32].

2.1. Goal & scope definition

The goal of this study is to assess the cradle-to-gate environmental impacts of co-transporting green hydrogen (H_2) and natural gas (NG) in existing NG pipelines with subsequent H_2 separation and compression via Electrochemical Hydrogen Compression (EHC). The environmental impacts of H_2/NG co-transport with EHC are compared to other promising H_2 transport options. To ensure a consistent comparison across all transport options, all environmental impacts are expressed relative to the so-called Functional Unit (FU). The FU is defined as "1 kg *high-purity hydrogen at end pressure* p_{end}" for all H_2 supply options.

H_2 end pressure levels p_{end} of 16 bar (only separation), 100 bar, 300 bar and 700 bar are considered to examine how EHC performs for different compression ratios. The end pressure levels of 100 bar and 300 bar are representative for requirements from industrial consumers [33], whereas 700 bar is the pressure level for H_2 refueling stations [34]. Furthermore, various volume percentages of H_2 during H_2/NG co-transport are considered, i.e., $x_{H2} = 5$, 10, 15, 20 and 50 vol.-%. Since EHC is not a mature technology yet, a base and optimistic case are modeled: The base case corresponds to operating conditions, which are reachable in the near future, whereas the optimistic case reflects target conditions for future development.

Fig. 1 gives an overview of the H_2/NG co-transport routes. In all co-transport routes, it is assumed that the H_2/NG mixture is transported from the production to the consumer site via a primary pipeline at operating pressure p_{op}. Afterwards, H_2 is separated from NG with one of the following two separation technologies: EHC and Pressure Swing Adsorption (PSA). While EHC includes compression of separated H_2 in a single device, PSA requires subsequent mechanical compression. We assume a H_2 purity after separation of at least 99.97 %, making it suitable for H_2 refueling stations [35].

The NG stream after the separation unit still contains a fraction of H_2 due to incomplete recovery. The NG stream including unrecovered H_2 is fed into a secondary pipeline at the operating pressure p_{sec}. Depending on the separation unit and the pressure of the secondary pipeline p_{sec}, further compression of the unrecovered stream might be required, which can result in increased energy demands [30].

When H_2 and NG are co-transported, a fraction of the pipeline capacity is used to transport H_2. We distinguish between two cases how this fraction of the pipeline capacity was used before transporting H_2:

1. **No excess capacity:** All available NG pipelines are fully used to transport NG. The fraction of the pipeline capacity now used to transport H_2 was previously used to transport NG. Hence, H_2 replaces NG which needs to be transported otherwise to still ensure that the NG demand is satisfied. We assume that a new pipeline segment needs to be built to transport the replaced NG, and corresponding environmental impacts from pipeline construction are considered.
2. **Excess capacity:** In this case, a fraction of the pipeline capacity is unused due to gradual phase-out of NG to reach defossilization targets. This unused pipeline capacity is now used to co-transport H_2 with NG. No new pipeline needs to be built.

For the comparison of the two separation and compression technologies (EHC vs. PSA incl. mechanical compression), we first consider a gate-to-gate system boundary for separation and compression of H_2 from the H_2/NG mixture (see Fig. 2). This narrow system boundary allows to understand the detailed energy demands and gate-to-gate GHG emissions.

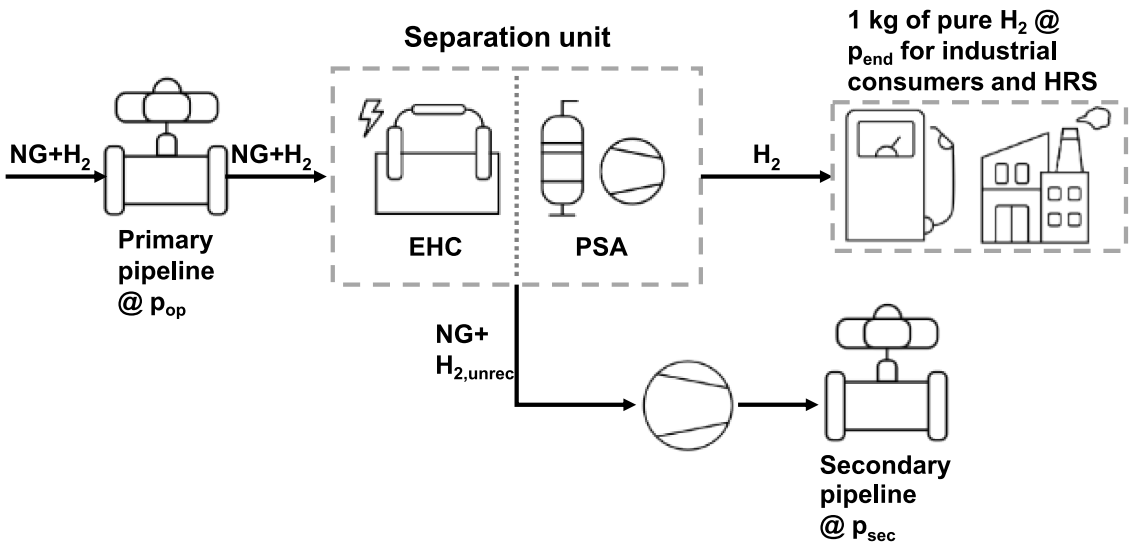

Fig. 1. Overview of hydrogen (H_2) and natural gas (NG) co-transport including the separation unit and H_2 consumer. The H_2/NG mixture is transported in the primary pipeline, which operates at operating pressure p_{op}. Then, the separation unit separates H_2 from the H_2/NG mixture such that the desired H_2 product at the desired end pressure level p_{end} exits the separation unit. As basis for comparison, we define a Functional Unit of 1 kg of high-purity H_2 at p_{end}. Since the separation units have incomplete H_2 recovery, the unrecovered H_2, together with the NG builds the unrecovered H_2/NG mixture, which is fed into a secondary pipeline operating at p_{sec}. EHC: Electrochemical Hydrogen Compression, PSA: Pressure Swing Adsorption including subsequent mechanical compression.

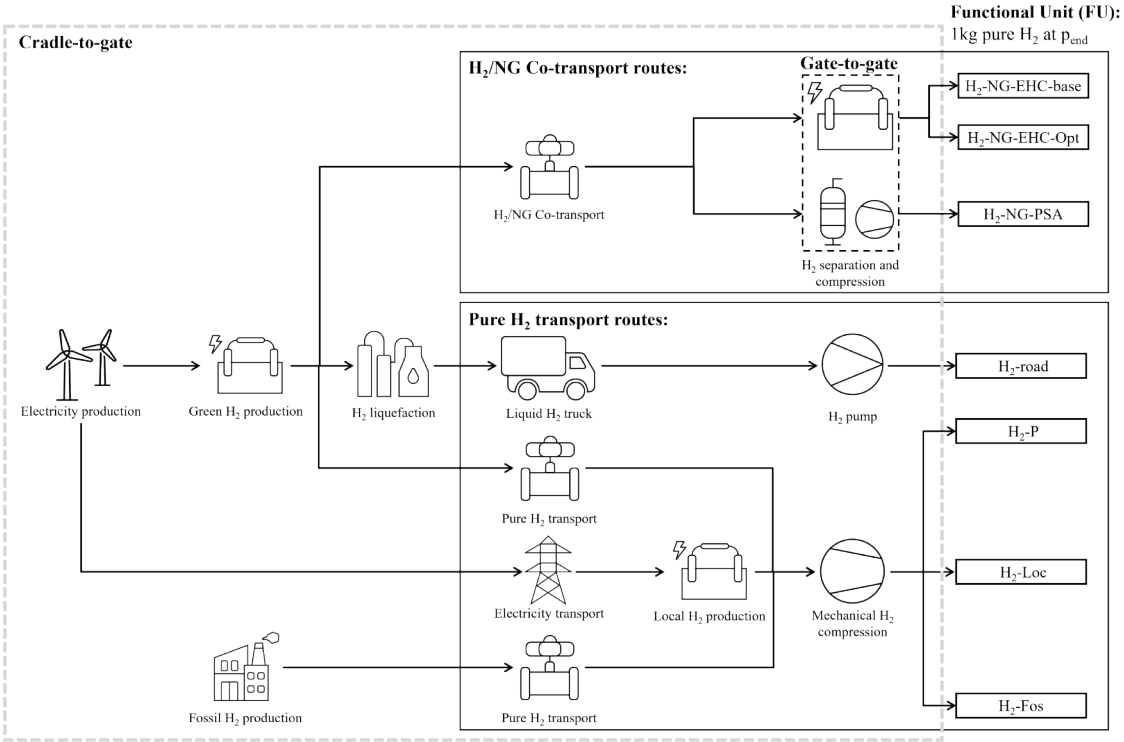

Fig. 2. Cradle-to-gate system boundary of the hydrogen (H_2) supply options. H_2-NG-EHC-base and H_2-NG-EHC-opt are transport routes where H_2 is co-transported in natural gas (NG) pipelines and then separated via Electrochemical Hydrogen Compression (EHC). Base and opt refer to the base and optimistic case of the EHC. H_2-NG-PSA describes H_2/NG co-transport with subsequent H_2 separation via Pressure Swing Adsorption (PSA). For the H_2/NG co-transport routes, we also define an alternative gate-to-gate system boundary to compare the two technologies for separation and compression. H_2–P describes H_2 transport in new pure H_2 pipelines, H_2-Road describes the transport of liquid H_2 in fuel-cell electric trucks and H_2-Loc describes the transport of electricity with subsequent decentralized H_2 production at the consumer site. H_2-Fos is the fossil benchmark where H_2 is produced via Steam Methane Reforming (SMR) and transported via H_2 pipelines. SMR: Steam Methane Reforming. p_{end}: End pressure of final H_2 product.

Since this study aims to assess several H_2 supply options, a second system boundary is chosen considering cradle-to-gate (see Fig. 2), which includes H_2 production and transport but excludes the use-phase and end-of-life. This study primarily assesses the environmental impacts of H_2/NG co-transport with EHC. To assess the environmental potential of EHC, a base model of EHC (**H_2-NG-EHC-base**) and an optimistic model

of EHC (**H_2-NG-EHC-opt**) are considered. As alternative technology for H_2 separation, PSA is included (**H_2-NG-PSA**). To evaluate whether H_2/NG co-transport is a promising option for H_2 supply, its environmental impacts are compared to four pure H_2 transport routes (see Fig. 2). These include green H_2 transport in new pure H_2 pipelines (**H_2–P**), transport of liquid H_2 via fuel cell electric-trucks (**H_2-Road**), transport of electricity, the decentral local production of green H_2 at the consumer-site (**H_2-Loc**) and the fossil production of H_2 via SMR and transport via H_2 pipelines (**H_2-Fos**).

As default, this study assumes a fixed transport distance of 1000 km and wind electricity from a representative wind farm in Northern Germany (see Section 2.1 in Supporting Information for details) as electricity source in the entire supply chain. This setup roughly represents transporting the renewable electricity from Northern Germany via H_2 to Southern Germany. Pure wind electricity as power supply is a best-case assumption, leading to the lowest possible impacts. For an electricity supply that is fully based on wind electricity, the environmental impacts are higher, as further components, such as storages are required for a reliable electricity supply [36].

An overview of all the considered parameter variations is given in Table 1.

Table 1
Overview of all considered parameter variations. H_2: Hydrogen, NG: natural gas, x_{H2}: Volume percentage of H_2 in H_2/NG mixture, p_{end}: End pressure of final H_2 product, p_{op}: Operating pressure of primary pipeline (see Fig. 1), p_{sec}: Operating pressure of secondary pipeline (see Fig. 1), Note a: Only separation.

Parameter	Type	Range/ Values	Relevance	Default Value(s)
End pressure of H_2 p_{end}	Discrete	16[a], 100, 300 and 700 bar	100 and 300 bar are representative for industrial consumers, while 700 bar is representative for H_2 refueling stations.	16 and 700 bar
Volume percentage of H_2 in H_2/NG mixture x_{H2}	Discrete	5, 10, 15, 20, 50 vol.-%	Up to 20 vol.-% possible today in German gas grids [37]. 50 vol.-% included as future reference.	20 vol.-%
Transport distance	Continuous	0-5000 km	Captures environmental trade-offs for varying transport distances.	1000 km
Global Warming Impact of electricity source in the supply chain	Continuous	0-450 g_{CO2}/kWh_{el}	Captures environmental trade-offs for various electricity impacts	Wind electricity (15 g_{CO2}/kWh_{el}, see Section 1.1 in SI)
Excess capacity	Discrete	Yes and no	Defines whether the fraction of the existing pipeline capacity used to transport H_2 during H_2/NG co-transport was previously utilized for pure NG transport or was available as excess capacity (see Section 2.1 and 2.2.4).	Yes
EHC model	Discrete	Base and Optimistic model (compare Section 2.2.8)	Included to reflect development targets as the EHC is not a mature technology yet	Both models included in transport routes (see Fig. 2)
Operating pressure of secondary pipeline p_{sec}	Discrete	1 and 16 bar	Injection of the unrecovered H_2/NG mixture of the separation unit into mid- (1 bar) or high-pressure (16 bar) distribution pipelines.	p_{sec} = 16 bar
Operating pressure of primary pipeline p_{op}	Discrete	16 and 100 bar	Transport of the H_2/NG mixture or pure H_2 in high-pressure distribution (16 bar) or long-distance transport pipelines (100 bar).	p_{op} = 16 bar

2.2. Life Cycle Inventory

The Life Cycle Inventory (LCI) comprises a foreground and background system. The foreground system consists of all modeled processes such as H_2 production and transport, while the background system covers all supporting processes such as raw material supply. All background processes are modeled using ecoinvent v3.9.1 [38]. In the following, the main parts of the foreground system are described, while a detailed overview of the data used can be found in the Supporting Information (SI).

2.2.1. Hydrogen production

Green H_2 production is modeled via Proton Exchange Membrane (PEM) electrolysis, where water is split into H_2 and oxygen using renewable electricity. An energetic efficiency of 70 % is assumed, based on literature data [39–42]. For the materials consumed in the construction of the electrolyzer, the near-future inventory from Bareiβ et al. [40] and Sharma et al. [41] is adopted. As a benchmark, fossil H_2 production via SMR, based on the LCI from Antonini et al. [43] is assumed. The full LCI data for fossil and green H_2 production can be found in Table 6-10 of the SI.

2.2.2. Hydrogen liquefaction

Liquefying H_2 is energy-intensive and a current field of research. The specific energy consumption ranges from 6 to 15 kWh/kg_{H2} [44–46], and thus, the average of 10.5 kWh/kg_{H2} is assumed. The construction of the liquefaction plant is modeled using the LCI data from Stolzenburg and Mubbala [47] with a plant lifetime of 30 years and a production capacity of 50 t_{H2}/d. The full LCI data can be found in Table 13 of the SI.

2.2.3. Mechanical hydrogen compression

For the construction of the H_2 compressor, the LCI data provided by Kanz et al. [48] for a 12 MW piston compressor with a lifetime of 50 years is assumed. As stated by Tahan [49], 0.5 % of H_2 is assumed to be lost during compression. The energy demands and the nominal power are calculated according to Khan et al. [50] (see Section 1.2 in the SI). The supply chain requires H_2 compressors in the pipelines, after the pipelines and between the electrolyzer and the pipelines. For the different compressor powers, the LCI from Kanz et al. [48] is scaled linearly. The full LCI data can be found in Tables 11 and 12 of the SI.

2.2.4. Pipeline transport

H_2 can be transported through existing NG pipelines with varying volume percentages of H_2. The H_2/NG mixture in the pipeline is modeled as an ideal gas mixture. As H_2 and NG are co-transported, the joint environmental impacts of co-transport need to be allocated to H_2 individually. To allocate the environmental impacts of H_2/NG co-transport, a consequential approach is applied.

In the consequential approach, the additional environmental impacts of co-transport of H_2 relative to transporting only NG are quantified. Through mixing H_2 with NG, the leakage rate, recompression energy and required maintenance during transport increase for the H_2/NG mixture compared to pure NG. These additional environmental impacts are attributed to H_2 transport during H_2/NG co-transport.

Furthermore, it is distinguished between two cases depending on how the fraction of the pipeline capacity was used prior to transporting H_2 during H_2/NG co-transport (see Fig. 3). In the *no excess capacity* case, it is assumed that the fraction of the pipeline capacity, which transports H_2 during H_2/NG co-transport was previously used to transport NG. Since the total NG supply to end users should remain constant even upon co-transporting H_2 with NG, a new pipeline segment needs to be built to transport that portion of NG that is replaced by H_2. The environmental impacts of constructing the new pipeline segment are included in our assessment (see Fig. 3 and Section 2.4 of the SI). In contrast, in the *excess capacity* case, it is assumed that the part of the pipeline capacity used to transport H_2 was previously unused due to ongoing defossilization and thus declining NG demand. In this case, the unused pipeline capacity transports H_2, while the NG demand is still fulfilled during H_2/NG co-transport. Consequently, no additional infrastructure is required, and only the aforementioned increased operational impacts resulting from H_2/NG co-transport are considered.

In addition to the consequential approach, an energy-based allocation of infrastructure impacts is analyzed in Section 2.4 of the SI. Both approaches yield similar results for all considered scenarios (see Fig. S8 in Section 3.2 of the SI), as the operational impacts are identical in both approaches and only the allocation of pipeline construction impacts differs.

The construction of new H_2 pipelines is modeled by accounting for the required amount of steel and the H_2 flow rate, in accordance to two technical reports of the JRC [38,51,52]. The lifetime of the new H_2 and H_2/NG co-transport pipelines is assumed to be 40 years, as modeled in the ecoinvent dataset for NG pipelines [38].

The leakage rate for H_2 in the co-transported pipelines is assumed to be the same as in the pure H_2 pipelines, i.e., 0.5 % per 1000 km [48]. For H_2/NG co-transport, this leakage rate represents a conservative upper bound for the H_2-attributable leakage. The leakage rate of a H_2/NG mixture is lower than that of pure H_2 due to the lower leakage rate of NG. Thus, only the H_2 fraction of the leaked gas would be attributed to H_2 transport, resulting in a lower bound for H_2 losses in the co-transported pipeline. However, the higher diffusivity of H_2 leads to preferential leakage through seals, enriching the leaked gas in H_2 relative to the H_2/NG composition in the co-transported pipeline. The real H_2-attributable leakage therefore lies between the allocated mixture leakage and the pure H_2 leakage rate assumed in our study. Additionally, it is accounted for an increase in pipeline maintenance equivalent to 2% of the natural gas pipeline's construction impacts due to the co-transport of H_2 [53,54]. For the pure H_2 pipelines, a 2% maintenance factor is applied to the H_2 pipeline construction [48,54,55].

Furthermore, for the pure H_2 transport and H_2/NG co-transport, the transport in two primary pipelines with different operating pressures p_{op} are considered (see Table 1). Recompression stations are required every 100 km along the H_2 pipelines to maintain operation. For the distribution pipelines, the compression from 11 to 16 bar requires 0.179 kWh/(100 km · kg_{H2}) [50]. The full LCI data for H_2/NG co-transport can be found in Tables 14–34, while the full LCI data for pure H_2 pipeline transport can be found in Tables 35–36 of the SI.

2.2.5. *Electricity transport*

Alternatively, to supply H_2, electricity could be transported in high-voltage alternating current (HVAC) transmission lines with the decentral production of H_2 at the consumer-site. The environmental impacts during the construction of the HVAC transmission lines are included in this study. The produced electricity from wind turbines is at high voltage, thus it is assumed that no additional transformers are needed.

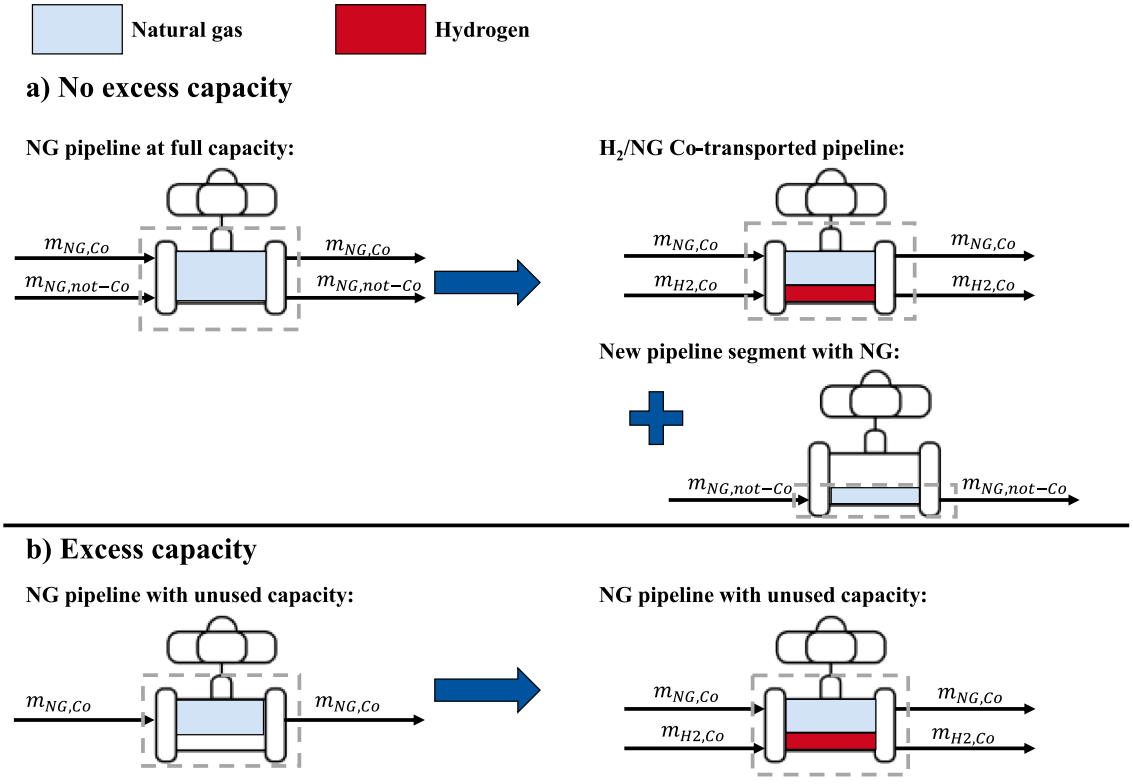

Fig. 3. System boundaries of hydrogen (H_2) and natural gas (NG) Co-transport in the a) No excess capacity and b) Excess capacity case. $m_{NG,not-Co}$: NG mass transported in the fraction of the pipeline capacity used to transport H_2 in the H_2/NG co-transported pipeline, $m_{NG,Co}$: NG mass transported with H_2 in the H_2/NG co-transported pipeline, $m_{H2,Co}$: H_2 mass transported during H_2/NG co-transport.

Losses of 1 %/100 km are assumed for the transmission [56]. The full LCI data is given in Table 37 of the SI.

2.2.6. Road transport

We choose 40 ton fuel-cell electric trucks for transporting the liquid H_2 via road. To model the truck construction, the LCI for fuel-cell electric trucks from Sacchi et al. [57] is modified such that the trucks transport liquid H_2 instead of compressed H_2 to achieve higher volumetric densities. To model the liquid H_2 tank, a ratio of 14.56 kg_{tank}/kg_{LH2} with the corresponding material demands from Weiszflog et al. [58] is assumed. The trucks have a lifespan of 710,000 km and an average load factor of 29 % [57]. The boil-off is assumed to be 0.1 %/d [58], while the trucks have an average truck speed of 80 km/h, with the truck travelling 800 km daily [57]. The full LCI data is given in Table 38 of the SI.

2.2.7. Hydrogen regasification & pumping

In contrast to the liquefaction of H_2, the regasification requires limited effort. Liquid H_2 is usually heated with ambient air or seawater, which results in exergy losses [59]. While technical options for recovering this exergy exist, they are not yet implemented [59]. Prior to heating, a cryopump pumps H_2 to the desired end pressure p_{end}, which reduces the energy demand compared to compressing gaseous H_2 [46,59]. H_2 losses of 0.5 % are assumed [49] and for the construction, the same nominal power and LCI as for the H_2 compressors is assumed. The full LCI data is given in Table 39 of the SI.

2.2.8. Hydrogen separation

For the H_2/NG co-transport routes (see Fig. 1), the inlet pressure for both separation units is 16 bar, which corresponds to the outlet pressure of the high-pressure distribution pipeline. We assume that the secondary pipeline can either be a high- or mid-pressure distribution pipeline. The mid-pressure distribution pipeline has an inlet pressure of 1 bar. For both separation units, it is assumed that 0.1 % of the H_2 is lost during the process for handling H_2 [52].

2.2.8.1. Electrochemical hydrogen compression. EHC consists of electrochemical cells, where H_2 and NG enter a flow-channel at the anode. Upon applying a voltage to the EHC, H_2 reacts to H+ ions and electrons at the anode, whereas NG is inert in the reaction at anode (see Fig. 4). The H+ ions migrate through the membrane to the cathode, where they recombine to molecular H_2 leading to a product stream with high H_2 concentration. Through pressurization of the cathode, the H_2 product has high pressures. Theoretically, high efficiencies at high pressures are reachable with EHC, however, cell irreversibilities, such as ohmic losses and H_2 back diffusion due to pressure gradients between cathode and anode lower the efficiencies in practice [14,18].

The overall energy demand of EHC consists of an electric energy demand needed for the electrochemical reactions, membrane and the theoretical minimum work of separation, of a heating demand required to heat the gases to stack temperature, and of a cooling demand to maintain the stack temperature [14,60]. The energy demands are obtained from a 1D simulation model in Modelica using the Software Dymola 2023x and the model library Hydrogen Energy Systems 3.14.0 (see Section 1.3 of SI). Due to the low maturity of EHC, a base case, which corresponds to near-future conditions and an optimistic case, which refers to future target conditions, is modeled. In the base case, voltage and faradaic efficiencies are calculated within the simulation model, accounting for ohmic, activation and H_2 back-diffusion losses. In both the base and optimistic case, EHC operates at a cell temperature of 40 °C with a cell area of 50 cm^2. The base case represents the simulation data of EHC with an operating current density of 1 A/cm^2 with H_2 recovery rates between 68 and 80 %. The optimistic case assumes that higher current densities of 2 A/cm^2 with recovery rates between 90 and 98 % can be reached, depending on the volume percentage of H_2 in the H_2/NG mixture [61] (see Table 2 and Section 1.3 of SI for details).

In the base case, it is assumed that the low-temperature heating demand above 40 °C is covered through a water-air heat pump powered by grid electricity. For the cooling demand, the use of cooling water from an unspecified natural origin is assumed, which is modeled as biosphere flow.

Since ohmic resistances dominate the voltage losses, a membrane with higher conductivity is assumed in the optimistic case leading to lower ohmic resistance (see Section 1.3 of SI). Additionally, the faradaic efficiency is set to 100 % in the optimistic case, assuming that no H_2 back-diffusion or incomplete reactions occur. The heating and cooling

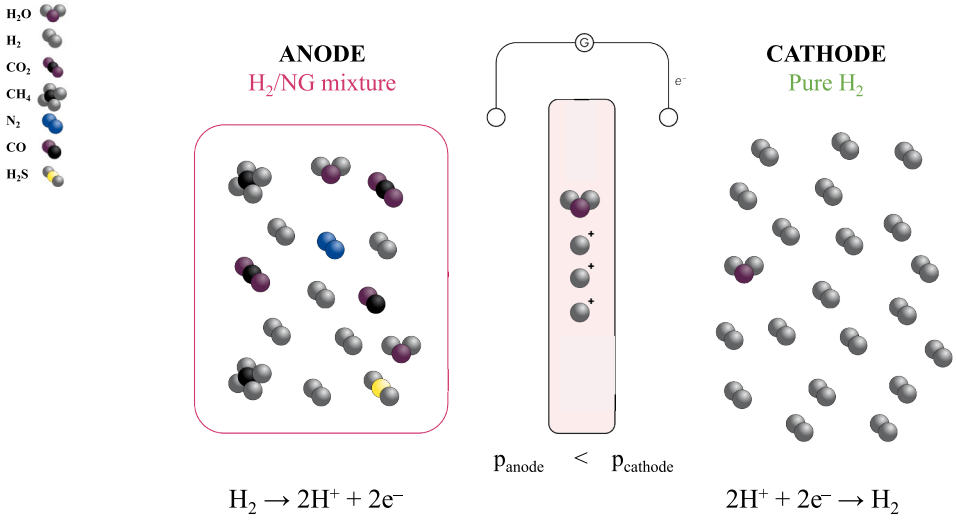

Fig. 4. Operation principle of Electrochemical Hydrogen Compression (EHC), adapted from Ref. [18]. The H_2/NG mixture is fed to the anode, where H_2 reacts to H+ ions. The H+ ions migrate through the proton-conducting membrane, while the components in NG are blocked. At the pressurized cathode, H+ ions recombine with electrons to form pure and compressed H_2. H_2: Hydrogen, NG: Natural gas, H_2O: Water, CO_2: Carbon dioxide, CH_4: Methane, N_2: Nitrogen, CO: Carbon monoxide, H_2S: Hydrogen sulfide, $p_{cathode}$: Cathode pressure, p_{anode}: Anode pressure.

Table 2
Main LCI data for Electrochemical Hydrogen Compression (EHC) with a feed gas containing 20 vol.-% H_2 for different H_2 end pressure levels p_{end}. The data for the other volume percentages are summarized in the SI. $w_{el,EHC}$: Electric energy demand of EHC, $w_{th,EHC}$: Heating demand of EHC, $w_{cool,EHC}$: Cooling demand of EHC. H_2: Hydrogen.

Parameter		Base	Optimistic	Sources
Lifetime [a]		7	10	[40,41]
Current density $\left[\frac{A}{cm^2}\right]$		1	2	own assumption
H_2 recovery rate [%]		68.5	92	own assumption, based on [61]
Only Separation	$w_{el,EHC}$ $\left[\frac{kWh}{kg_{H2}}\right]$	11.38	6.24	Values obtained from 1D simulation model. In optimistic case, the model is adapted for novel membrane material and no faradaic losses (see Section 1.3 in SI).
	$w_{th,EHC}$ $\left[\frac{kWh}{kg_{H2}}\right]$	1.69	1.69	Values obtained from 1D simulation model
	$w_{cool,EHC}$ $\left[\frac{kWh}{kg_{H2}}\right]$	12.05	12.05	Values obtained from 1D simulation model
100 bar	$w_{el,EHC}$ $\left[\frac{kWh}{kg_{H2}}\right]$	12.18	6.9	Values obtained from 1D simulation model. In optimistic case, the model is adapted for novel membrane material and no faradaic losses (see Section 1.3 in SI).
	$w_{th,EHC}$ $\left[\frac{kWh}{kg_{H2}}\right]$	1.53	1.53	Values obtained from 1D simulation model
	$w_{cool,EHC}$ $\left[\frac{kWh}{kg_{H2}}\right]$	12.56	12.56	Values obtained from 1D simulation model
300 bar	$w_{el,EHC}$ $\left[\frac{kWh}{kg_{H2}}\right]$	12.73	7.29	Values obtained from 1D simulation model. In optimistic case, the model is adapted for novel membrane material and no faradaic losses (see Section 1.3 in SI).
	$w_{th,EHC}$ $\left[\frac{kWh}{kg_{H2}}\right]$	1.44	1.44	Values obtained from 1D simulation model
	$w_{cool,EHC}$ $\left[\frac{kWh}{kg_{H2}}\right]$	13.12	13.12	Values obtained from 1D simulation model
700 bar	$w_{el,EHC}$ $\left[\frac{kWh}{kg_{H2}}\right]$	13.38	7.6	Values obtained from 1D simulation model. In optimistic case, the model is adapted for novel membrane material and no faradaic losses (see Section 1.3 in SI).
	$w_{th,EHC}$ $\left[\frac{kWh}{kg_{H2}}\right]$	1.47	1.47	Values obtained from 1D simulation model
	$w_{cool,EHC}$ $\left[\frac{kWh}{kg_{H2}}\right]$	13.77	13.77	Values obtained from 1D simulation model

demands are assumed to be the same as in the base case. However, the heating demand is covered by available waste heat, thereby assuming no additional environmental burdens for heat supply. The cooling demand is met with cooling water, modeled the same as in the base case.

For the material demands of the EHC, the same materials as for a PEM electrolyzer are assumed with the only exception that the anode catalyst is platinum for EHC instead of iridium for PEM. The same inventory as Sharma et al. [41] and Bareiβ al. [40] is assumed as they provide a base and optimistic case for the material demands of the PEM electrolyzer. The LCI data is summarized in Table 2Table 40-Table 45 of the SI of the SI.

2.2.8.2. Pressure Swing Adsorption. PSA is an established technology for H_2 separation from reforming gases and is currently used in the chemical and petroleum refining industry [17,62]. Typically, the feed consists of high volumetric concentration of H_2 (>70 vol.-%) [16], thus using PSA for the separation of H_2 from NG at low concentrations is not conventional. In the PSA, methane and other heavy gases in NG are adsorbed in the column so that a purified H_2 stream passes through the column. In this work, a PSA process in accordance to Dehdari et al. [16] is assumed, which consists of six columns and twelve steps in each cycle. A higher number of columns is necessary to facilitate the pressure equalization steps, which increase the H_2 recovery for lower H_2 concentrations in the feed stream [16].

The choice of the adsorbents in the PSA system are crucial for the operational performance. In accordance to Dehdari et al. [63], a pre-layer of silica gel to adsorb heavy hydrocarbons and CO_2, activated carbon to adsorb methane and zeolite in a post-layer to adsorb nitrogen is chosen.

One challenge for PSA systems is to maximize both H_2 recovery and purity [16,63,64]. Typically, PSA can achieve H_2 purities in the range of 98–99.999 %, with a H_2 recovery rate between 70 and 90 % [64,65], with recent work suggesting high recoveries of >80% for high purity H_2 (>99%) [16]. The recovery rates are taken from Dehdari et al. [16], who provide recovery rates for 5-30 vol.-% H_2. However, two adjustments are made: First, it is assumed that the purity requirements for fuel cells of >99.97 % are met in each case and second, since the authors do not provide values for 50 vol.-%, it is assumed that the recovery rate achieved for 30 vol.-% H_2 can also be achieved for 50 vol.-%.

The energy demand for the PSA includes the compression of the H_2 product stream to the desired end pressure p_{end} and of the unrecovered H_2/NG mixture to the operating pressure of the secondary pipeline p_{sec} (see Fig. 1). Since the desorption pressure of the PSA is 1 bar, the unrecovered H_2/NG mixture could be directly fed into a mid-pressure distribution pipeline operating at $p_{sec} = 1$ bar. Otherwise, if the unrecovered H_2/NG mixture is fed back into the high-pressure distribution pipeline with $p_{sec} = 16$ bar, the unrecovered mixture stream needs to be compressed as well, leading to higher energy demands (see Section 1.2 of SI). Both cases for the unrecovered H_2/NG mixture are considered in this analysis.

For the construction of the PSA, the demand of stainless steel for the valves and columns and the material demands of the adsorbents are included. All material demands for the PSA system are taken from Dehdari et al. [63]. Selected LCI parameters for the PSA are summarized in Table 3, while the full LCI data can be found in Table 51 of the SI.

2.3. Life Cycle Impact Assessment

We use Environmental Footprint (EF) v3.1 [31] to translate the biosphere flows into environmental impacts. As recommended by the Joint Research Center (JRC) of the European Commission, we include 16 different environmental impact categories in our analysis to assess the risk of environmental burden-shifting [31]. However, according to EF v3.1, the *GWP100* characterization factor of H_2 is 0, whereas recent studies show that H_2 could form methane or other greenhouse gases in the atmosphere and is therefore also associated with a characterization factor [66]. Studies show that the characterization factor of H_2 for *GWP100* ranges from 5 to 12 [66–69]. We follow the results of Sand et al. and assume a *GWP100* characterization factor of 11.6 for H_2 [66].

3. Results

This section is divided into three subsections. In the first subsection, we focus on detailed analyses of the environmental impacts of H_2 separation and compression (see Fig. 2). In the second subsection, we compare the cradle-to-gate environmental impacts of H_2/NG co-transport with subsequent H_2 separation and compression to the alternative pure H_2 transport routes (see Fig. 2). In the third subsection, we discuss our findings.

3.1. Analysis of hydrogen separation and compression

In Section 3.1.1, we analyze the electricity demand and Global Warming Impact (GWI) of H_2 separation and compression via EHC and PSA, but without considering the other supply chain steps (gate-to-gate system boundary in Fig. 2). In Section 3.1.2, we analyze the cradle-to-gate GWI of H_2/NG co-transport with H_2 separation and compression for various volume percentages of H_2 in the H_2/NG mixture.

3.1.1. Electricity demand and Global Warming Impact of hydrogen separation and compression

For 20 vol.-% H_2, the base model of EHC consumes 11.4-13.4 kWh/kg_{H2} (see Fig. 5a). Changing the membrane material such that EHC has lower ohmic and H_2 back-diffusion losses (see Section 1.3 of SI) halves the electricity demand in the optimistic case compared to the base case. The electricity demand of PSA depends on the pipeline into which the unrecovered H_2 and NG are fed. If the unrecovered H_2/NG mixture remains at the desorption pressure of 1 bar, the unrecovered H_2/NG mixture can be fed into a mid-pressure distribution pipeline without additional compression. In this case, both the base and optimistic model of EHC consume more electricity than PSA (see Fig. 5a, $p_{sec} = 1$ bar). On the other hand, if the unrecovered H_2/NG mixture is fed into a high-pressure distribution pipeline, the unrecovered H_2/NG mixture needs to be compressed from 1 to 16 bar. In this case, electricity demand of the PSA ranges from 7.2 to 9.6 kWh/kg_{H2} and is higher than the optimistic model of EHC (see Fig. 5a, $p_{sec} = 16$ bar). For EHC, no compression of the unrecovered H_2/NG mixture is needed as it exits EHC at inlet pressure, i.e., 16 bar.

To validate our results, we compare our modeled EHC energy demands to literature. For H_2 compression with atmospheric inlet pressure, Lipp achieves energy demands of 3-12 kWh/kg_{H2} for compression up to 207 bar and 20 kWh/kg_{H2} for compression up to 81.6 MPa [14,70]. Prokopou et al. [21] report energy demands of 11.7–17.2 kWh/kg_{H2} for compression to 10–700 bar at 1 A/cm^2. For H_2 separation, Jackson et al. [71] report 3.5–12.5 kWh/kg_{H2} at 0.2 A/cm^2, while Nordio et al. [72] report 3.72 kWh/kg_{H2} for H_2 separation at 6 bar inlet pressure. Mrusek et al. [60] determine a thermal energy demand of 5.6–7.0 kWh/kg_{H2} for gas heating and humidification, consistent with the heating demands in our model (see Table 5 of SI). Our base model has an electricity demand of 11.4–13.4 kWh/kg_{H2}, which is comparable with these studies. Lower energy demands in our study compared to Prokopou et al. [21] mainly result from the higher inlet pressure in our system, which reduces the compression ratio. Our optimistic model (5.7–8.1 kWh/kg_{H2}) is comparable to Dale et al., who report an energy demand of 7.5 kWh/kg_{H2} for compression up to 138 bar [73]. The assumed improved membrane properties in our optimistic EHC model are supported by experimental demonstrations of Giner ELX Inc. who used a modified membrane with low H_2 back-diffusion to achieve an energy consumption of 2.0 kWh/kg_{H2} at 350 bar end pressure [14,74].

For 20 vol.-% H_2, the gate-to-gate GWI of EHC-opt ranges from 0.1 to 0.12 $kg_{CO2\text{-}eq}$/kg_{H2}, which is lower than that of the PSA (0.13-0.21 $kg_{CO2\text{-}eq}$/kg_{H2}) for all considered end pressures if the unrecovered H_2/NG mixture is compressed to 16 bar (see Fig. 5b). If the unrecovered H_2/NG mixture remains at 1 bar, EHC-opt has a higher GWI than PSA (0.03-0.11 $kg_{CO2\text{-}eq}$/kg_{H2}) for all considered end pressures. The GWI of EHC-base ranges from 0.29 to 0.31 $kg_{CO2\text{-}eq}$/kg_{H2}, which is higher than that of PSA in all end pressure cases because of the high energy demand during separation and compression. For only separation ($p_{end} = 16$ bar), the material impacts of EHC-base are twice as high as those of PSA. For higher compression ratios, the material impacts of EHC-base and PSA are similar because the PSA system requires an additional compressor for the H_2 product, which is not needed in the case of only separation.

For lower volume percentages of H_2 in the H_2/NG mixture and $p_{sec} = 16$ bar (see Fig. S3 in SI), the amount of NG in the unrecovered H_2/NG mixture of PSA increases, leading to an increased electricity demand for compression (32.7-35.1 kWh/kg_{H2} for 5 vol.-% H_2 and 16.4-18.8 kWh/kg_{H2} for 10 vol.-% H_2) and an increased GWI (0.47-0.55 $kg_{CO2\text{-}eq}$/kg_{H2} for 5 vol.-% H_2 and 0.25-0.33 kWh/kg_{H2} for 10 vol.-% H_2). Consequently, for 5 and 10 vol.-% H_2, the GWI of both EHC-base (0.43-0.45 $kg_{CO2\text{-}eq}$/kg_{H2} for 5 vol.-% H_2 and 0.33-0.35 kWh/kg_{H2} for 10 vol.-% H_2) and EHC-opt (0.11-0.13 $kg_{CO2\text{-}eq}$/kg_{H2} for 5 vol.-% H_2 and 0.1-0.12 kWh/kg_{H2} for 10 vol.-% H_2) is lower or comparable to that of PSA.

3.1.2. Global Warming Impact of hydrogen and natural gas co-transport including hydrogen separation and compression

In Fig. 6, we depict the cradle-to-gate GWI for H_2/NG co-transport with subsequent separation via PSA and EHC, including H_2 production; using different volume percentages of H_2 in the H_2/NG mixture and default values for variable parameters (see Table 1). The results for the long distance ($p_{op} = 100$ bar) yield similar results as high-pressure distribution pipelines ($p_{op} = 16$ bar) and are therefore included in Fig. S4 of the SI.

With increasing volume percentage x_{H2} of H_2, the cradle-to-gate GWI

Table 3
Main LCI data for Pressure Swing Adsorption with a feed gas containing 20 vol.-% H_2 for H_2 end pressure levels p_{end}. H_2: Hydrogen. p_{sec}: Pressure level of the unrecovered H_2 and natural gas mixture (see Fig. 1).

Parameter [unit]	Value		Sources
Lifetime [a]	40		[63]
H_2 recovery rate [%]	80.84		[16]
Parameter [unit]	$p_{sec} = 1$ bar	$p_{sec} = 16$ bar	
Lifetime [a]	40	40	[63]
H_2 recovery rate [%]	80.84	80.84	[16]
$w_{el}\left[\frac{kWh}{kg_{H2}}\right]$, only separation	0	7.22	[50]
$w_{el}\left[\frac{kWh}{kg_{H2}}\right]$, 100 bar	0.975	8.195	[50]
$w_{el}\left[\frac{kWh}{kg_{H2}}\right]$, 300 bar	1.63	8.85	[50]
$w_{el}\left[\frac{kWh}{kg_{H2}}\right]$, 700 bar	2.39	9.61	[50]

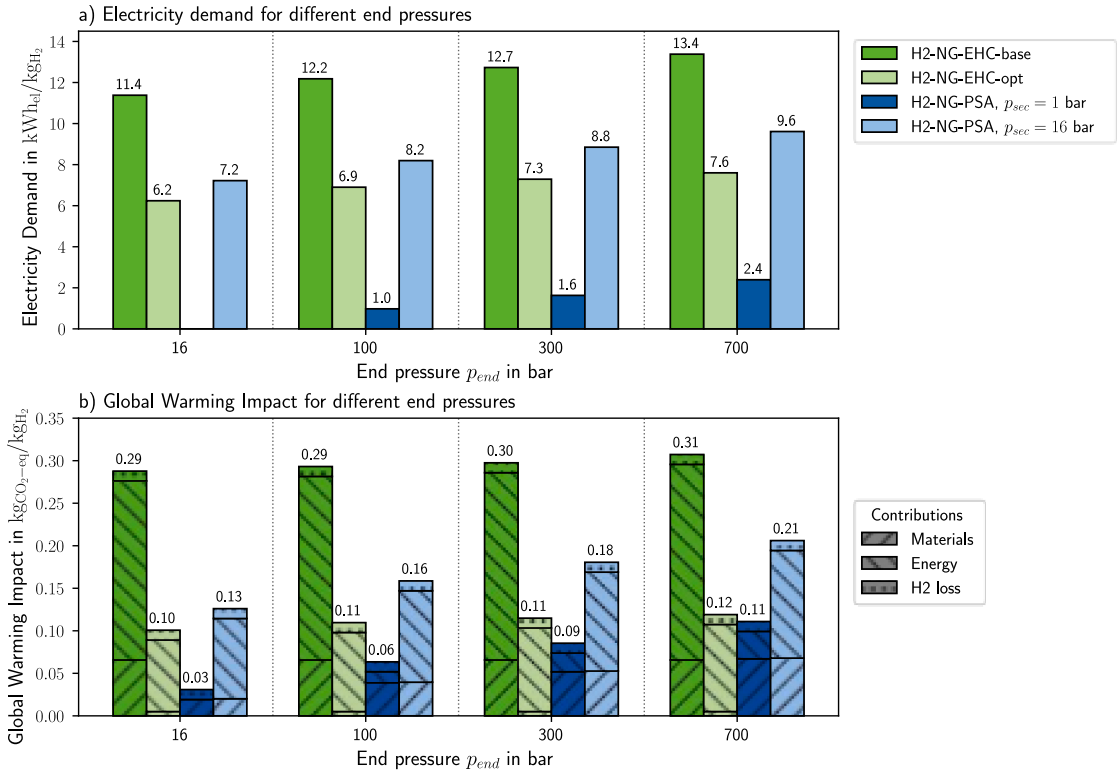

Fig. 5. Overview of the gate-to-gate electricity demands and Global Warming Impact (GWI) for separation and compression via the Electrochemical Hydrogen Compression (EHC) and Pressure Swing Adsorption (PSA) combined with mechanical compression. The transport distance is 0 km. The volume percentage of H_2 x_{H2} is 20 vol.-%. p_{sec}: Pressure level of the unrecovered hydrogen and natural gas mixture (see Fig. 1). p_{end}: End pressure of the H_2 product. In H_2-NG-EHC-base and H_2-NG-EHC-opt, H_2 is separated via EHC. Base and opt refer to the base and optimistic case of EHC. In H_2-NG-PSA, H_2 is separated via PSA. H_2: Hydrogen.

decreases in all cases (see Fig. 6). The decreasing GWI with increasing volume percentage x_{H2} for H_2/NG co-transport with EHC-base is caused by decreasing electricity and heating demands. For H_2/NG co-transport with EHC-opt, the changes in the GWI are minor as the heating demands are met through available waste heat. As discussed in Section 3.1.1, a lower volume percentage x_{H2} increases the GWI of the PSA if the unrecovered H_2/NG mixture is compressed to 16 bar. H_2/NG co-transport with EHC-opt has a lower or similar GWI as PSA for all considered cases. EHC-opt is more favorable than PSA for H_2 separation and compression to 700 bar ($p_{end} = 700$ bar) than for only separation ($p_{end} =$ 16 bar), as the PSA operates at 16 bar and no additional mechanical compressor is required for the H_2 product. EHC can separate and compress H_2 in one device, making it more favorable for higher compression ratios.

Furthermore, we distinguish whether the portion of the existing pipeline used to transport H_2 during H_2/NG co-transport was previously utilized for pure NG transport or was available as excess capacity (see Section 2.1 and 2.2.4). An excess capacity in the original NG pipeline results in lower GWI due to lower construction impacts, while the overall trend in the GWI across the considered separation technologies and H_2 volume percentages remains consistent in both cases (see Fig. S4 of the SI).

While H_2/NG co-transport with PSA can achieve low GWI under ideal conditions ($p_{sec} = 1$ bar), this setup assumes that the unrecovered H_2/NG mixture does not require recompression, which is typically incompatible with pipeline injection requirements of higher pressures for safe and efficient H_2 transport. As a result, the recompression of the unrecovered H_2/NG mixture of the PSA is necessary ($p_{sec} = 16$ bar), increasing electricity demand and GWI, particularly at low H_2 volume percentages. In contrast, EHC offers greater flexibility: It can achieve low GWI at all H_2 volume percentages x_{H2} and it can operate at high inlet pressures, eliminating the need for additional compression of the unrecovered H_2/NG mixture. While both EHC and PSA show competitive GWI for H_2 separation and compression, EHC offers greater integration flexibility into existing pipeline systems and has the potential of achieving lower GWI than the PSA system (see Figs. 5 and Fig. 6).

3.2. Comparison of hydrogen and natural gas co-transport to other hydrogen transport routes

In this subsection, we compare H_2/NG co-transport with EHC to the alternative pure H_2 transport routes (see Fig. 2). We first present a contribution analysis of the GWI in Section 3.2.1, followed by an analysis of environmental burden-shift in Section 3.2.2. In Section 3.2.3, we conduct a sensitivity analysis of the GWI for the electricity in the supply chain and the transport distance.

3.2.1. Contribution analysis

H_2/NG co-transport with EHC has the potential to achieve a GWI that is lower than or equal to all other H_2 transport routes despite the additional energy-intensive separation and compression of H_2 (see Fig. 7).

If only separation is considered ($p_{end} = 16$ bar), all H_2/NG co-transport routes have higher impacts from separation and compression than pure H_2 transport routes as these do not require additional separation. Thus, if $p_{end} = 16$ bar, pure H_2 pipelines have the lowest GWI, followed by H_2/NG co-transport with EHC-opt (see Fig. 7a). If separation and compression to 700 bar is considered ($p_{end} = 700$ bar), H_2/NG co-transport with EHC-base or PSA have higher impacts from separation and compression than pure H_2 transport routes. For H_2/NG co-transport with EHC-opt, these impacts are comparable or even lower than in the pure H_2 transport routes due to improvements in material usage and energetic efficiency of EHC. Thus, for $p_{end} = 700$ bar, H_2/NG co-transport with EHC-opt has the lowest GWI, followed by pure H_2

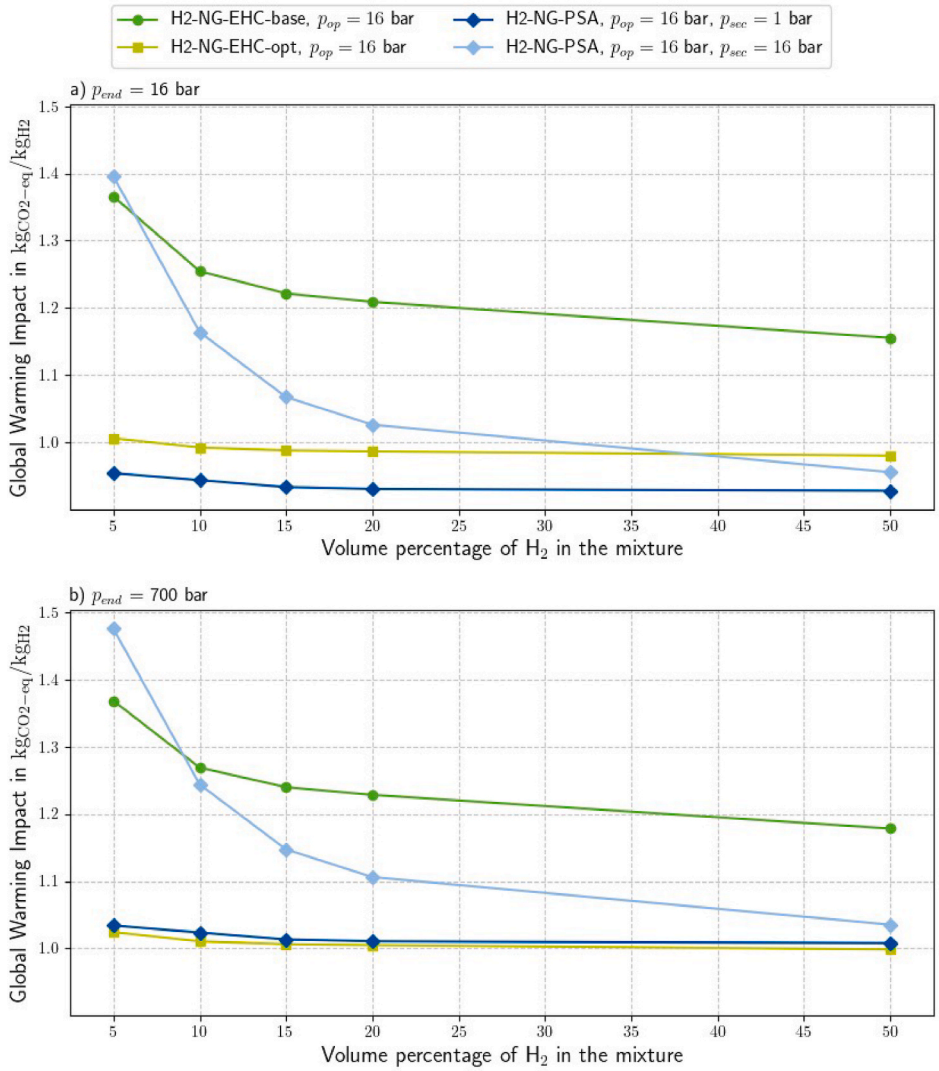

Fig. 6. Sensitivity analysis of the Global Warming Impact (GWI) with respect to the volume percentage of hydrogen (H_2) x_{H2}. The transport distance is 1000 km. We assume that the fraction of the pipeline capacity used to transport H_2 during H_2/NG co-transport was previously unused and available as excess capacity (see Table 1). p_{sec} : Operating pressure of the secondary pipeline (see Fig. 1). p_{op}: Operating pressure of the primary pipeline (see Fig. 1). p_{end}: Final pressure of the H_2 product. The subplot a) shows only separation at 16 bar, whereas the subplot b) shows the case of separation and compression to 700 bar. H_2-NG-EHC-base and H_2-NG-EHC-opt are transport routes where H_2 is co-transported with natural gas (NG) in NG pipelines and then separated via Electrochemical Hydrogen Compression (EHC). Base and opt refer to the base and optimistic case of the EHC. In H_2-NG-PSA, H_2 is co-transported with NG but subsequently separated via Pressure Swing Adsorption (PSA).

pipelines (see Fig. 7b). In both end pressure cases, the GWI of H_2/NG co-transport with EHC-opt is lower than that with PSA. H_2/NG co-transport with EHC-base has a higher GWI than with PSA but similar GWI as local H_2 production and a lower GWI than transport of liquid H_2 via trucks.

If the original NG pipeline had an excess capacity for H_2 co-transport, the infrastructure impacts are lower than for pure hydrogen pipelines because no new pipeline segment is necessary. If the existing NG pipeline had no excess capacity for H_2 co-transport, a new pipeline segment needs to be built to transport the amount of NG that is replaced by H_2. In this case, the infrastructure impacts of H_2/NG co-transport and pure hydrogen pipelines are comparable, and the ranking between these routes depends primarily on the separation and compression impacts. Under both assumptions, H_2/NG co-transport with EHC-opt has a lower GWI than pure H_2 pipelines at $p_{end} = 700$ bar. At $p_{end} = 16$ bar, pure H_2 pipelines have a lower GWI than H_2/NG co-transport under both assumptions, as no additional separation and compression is required for pure H_2 pipelines. For EHC-base, the excess capacity assumption can change the ranking relative to electricity transport and local H_2 production (H_2-Loc): without excess capacity, EHC-base has a higher GWI than H_2-Loc at $p_{end} = 16$ bar, while at $p_{end} = 700$ bar, EHC-base has a lower GWI. With excess capacity, EHC-base achieves a lower GWI than H_2-Loc at both end pressures (see Fig. 7).

To validate our LCA results, we compare our results to published values for known H_2 transport routes. For pure H_2 pipeline transport, Wulf et al. [55] determine a GWI of 1.5–1.7 $kg_{CO2\text{-}eq}/kg_{H2}$ at 700 bar end pressure over distances up to 400 km, Akhtar et al. [7] obtain 1.57 $kg_{CO2\text{-}eq}/kg_{H2}$ for a 300 km pipeline and 700 bar end pressure, and De Kleijne et al. [39] find that pipeline transport alone adds 1.5 $kg_{CO2\text{-}eq}/kg_{H2}$ for a distance of 1000 km and an end pressure of 80 bar. While the results of Wulf et al. [55] and Akhtar et al. [7] are comparable to our results (see Fig. 7), De Kleijne et al. [39] find that the GWI during pipeline transport is higher than our cradle-to-gate GWI including production. This large difference arises because they assume that the electricity they use for recompression has a GWI of 37 $g_{CO2\text{-}eq}$/kWh, which is more than twice as high as compared to wind electricity in our study. For liquid H_2 transport via trucks, Akhtar et al. [7] obtain 2.08 $kg_{CO2\text{-}eq}/kg_{H2}$

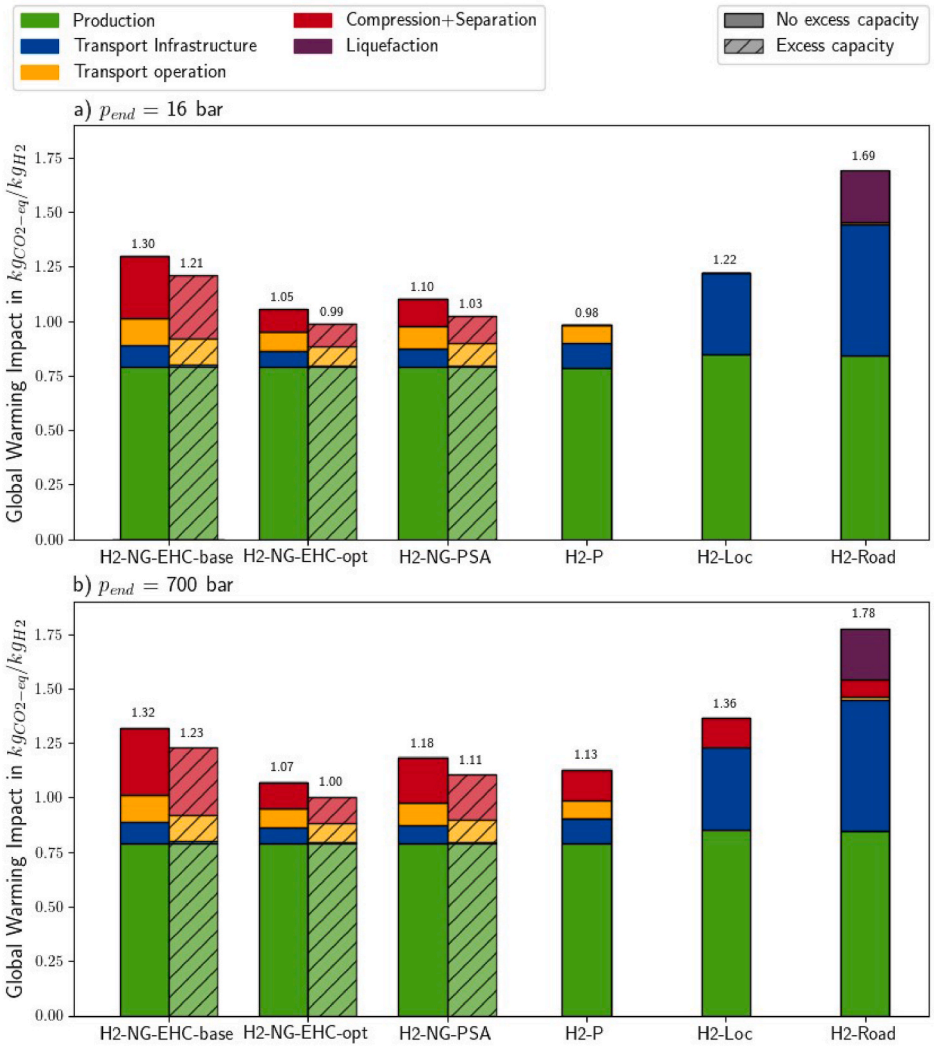

Fig. 7. Contribution analysis comparing the GWI of hydrogen (H_2) and natural gas (NG) co-transport in high-pressure distribution pipelines to the alternative H_2 transport routes for 20 vol.-% H_2 and p_{sec} = 16 bar. The transport distance is 1000 km. H_2-NG-EHC-base and H_2-NG-EHC-opt are transport routes where H_2 is co-transported with NG and then separated via Electrochemical Hydrogen Compression (EHC). Base and opt refer to the base and optimistic case of the EHC. In H_2-NG-PSA, H_2 is co-transported with NG but subsequently separated via Pressure Swing Adsorption (PSA). H_2–P describes H_2 transport in pure H_2 pipelines, H_2-Loc describes the transport of electricity with subsequent decentral H_2 production at the consumer-site and H_2-Road describes the transport of liquid H_2 in fuel-cell electricic trucks. GWI: Global Warming Impact. p_{end}: Final pressure of the H_2 product, p_{sec} : Operating pressure of the secondary pipeline (see Fig. 1).

for truck transport over 400 km. For H_2/NG co-transport with PSA, Di Lullo et al. [30] determine substantially higher values, with hydrogen separation alone adding 4.6–8.2 $kg_{CO2\text{-}eq}/kg_{H2}$. This large difference is mainly due to their use of fossil H_2 and carbon-intensive grid electricity, compared to green H_2 with wind electricity in our study. Overall, our results are comparable to the existing literature, while remaining differences are attributable to differing electricity assumptions and impact assessment methods.

Our results show that H_2/NG co-transport with EHC-opt maintains a lower GWI than most other transport options, including pure H_2 pipelines for compression up to 700 bar. Even if only separation is considered, H_2/NG co-transport with EHC-opt has a comparable GWI as pure hydrogen pipelines. However, wind electricity is assumed as electricity source, which leads to low electricity impacts despite high electricity demands for the separation and compression. A variation of the GWI for the electricity used in the supply chain is shown in Section 3.2.3. A contribution analysis for other volume percentages of H_2 in the H_2/NG mixture is given in Figs. S5–S7 of the SI.

3.2.2. Analysis of environmental burden-shift

While the green H_2 transport routes can reduce the GWI compared to fossil H_2, it is essential to assess whether these GWI reductions come at the cost of increased impacts in other environmental categories. Therefore, fossil H_2 serves as baseline to quantify this environmental burden-shift. All considered H_2 transport routes have lower impacts than the fossil reference in four to seven environmental categories (see Fig. 8). H_2/NG co-transport with EHC-opt or PSA and transport in pure H_2 pipelines reduce the environmental impacts in the categories climate change, resource depletion of energy resources (RD_e), ozone depletion (OD), photochemical oxidant formation (PCOF), eutrophication of terrestrial (E_t), acidification (A_{tfw}) and eutrophication marine (E_m) compared to the fossil reference. Among those seven environmental impact categories, H_2/NG co-transport with EHC-base, the local production of H_2 (H_2-Loc) and liquid H_2 transport via trucks (H_2-Road) have higher impacts than the fossil reference in A_{tfw} and E_m, while H_2-Road also exceeds the impacts in E_t. Our results therefore show that the green H_2 transport routes have higher impacts than the fossil reference in at least nine out of sixteen environmental categories. Consequently, compared to the fossil reference, the environmental impacts in the

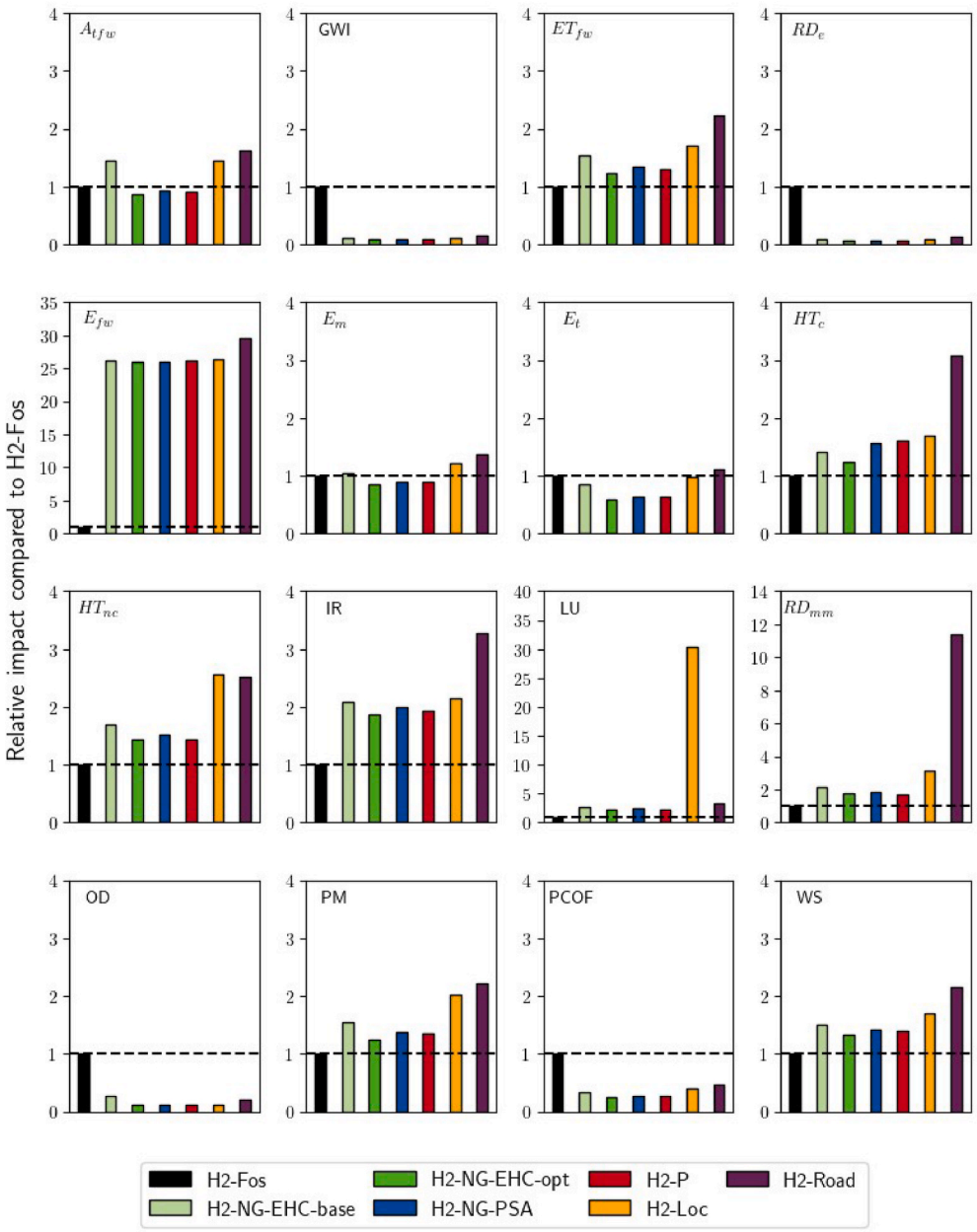

Fig. 8. Relative environmental impact of the green hydrogen (H_2) transport routes compared to the fossil reference (H_2-Fos) in all 16 impact categories for p_{sec} = 16 bar and 20 vol.-% H_2. The final pressure of H_2 is p_{end} = 700 bar. The transport distance is 1000 km. We assume that the fraction of the existing pipeline capacity used to transport H_2 during H_2/NG co-transport was previously unused and available as excess capacity (see Table 1). p_{end}: Final pressure of the H_2 product, p_{sec} : Operating pressure of the secondary pipeline (see Fig. 1). A_{tfw}: Acidification, GWI: Global Warming Impact, ET_{fw}: Ecotoxicity of freshwater, RD_e: Resource depletion of energy resources, E_{fw}: Eutrophication of freshwater, E_m: Eutrophication of marine, E_t: Eutrophication of terrestrial, HT_c: Human toxicity carcinogenic, HT_{nc}: Human toxicity non-carcinogenic, IR: Ionizing radiation, LU: Land use, RD_{mm}: Resource depletion of metals and minerals, OD: Ozone depletion, PM: Particulate matter formation, PCOF: Photochemical oxidant formation, WS: Water use. H_2-NG-EHC-base and H_2-NG-EHC-opt are transport routes where H_2 is co-transported with natural gas (NG) and then separated via Electrochemical Hydrogen Compression (EHC). Base and opt refer to the base and optimistic case of the EHC. In H_2-NG-PSA, H_2 is co-transported with NG but subsequently separated via Pressure Swing Adsorption (PSA). H_2–P describes H_2 transport in pure H_2 pipelines, H_2-Loc describes the transport of electricity with subsequent decentral H_2 production at the consumer-site and H_2-Road describes the transport of liquid H_2 in fuel-cell electricic trucks. H_2-Fos is the fossil benchmark where H_2 is produced via Steam Methane Reforming (SMR) and transported via H_2 pipelines. (For interpretation of the references to colour in this figure legend, the reader is referred to the Web version of this article.)

category climate change are decreased through green H_2 transport routes, however, the environmental impacts in other categories are increased, so-called environmental burden-shift.

The nine impact categories, in which the green H_2 transport routes exceed the fossil reference are: Ecotoxicity (ET_{fw}), eutrophication freshwater (E_{fw}), human toxicity carcinogenic (HT_c), human toxicity non-carcinogenic (HT_{nc}), ionizing radiation (IR), land use (LU), resource depletion of metals and minerals (RD_{mm}), particulate matter formation (PM) and water use (WS). The increase in all mentioned environmental impact categories except E_{fw} and WS are mainly influenced by the increased electricity demand for green compared to fossil H_2 production. The main driver for the increase in E_{fw} and WS is the high demand of deionized water for electrolytic H_2 production. The high demand for deionized water also contributes to the increase in the environmental impacts of ET_{fw} and IR. Besides the increased electricity demand, the material demands for the stack and BoPs of the electrolyzer and EHC

also increase the environmental impact in RD_{mm} and A_{tfw}. For H_2-Loc, the construction of the transmission networks significantly increases the impacts in LU. For H_2-Road, the environmental impacts are the highest because of the high material requirements for vehicle production, in particular the production of liquid H_2 tanks.

Overall, the extent of environmental burden-shift varies among the green H_2 transport routes, with H_2/NG co-transport with EHC-opt and pure H_2 pipelines showing lower impacts than the fossil reference in seven out of sixteen categories. H_2/NG co-transport with EHC-opt achieves comparable or lower impacts than PSA in all categories, as the avoided mechanical compression reduces material and energy demands. However, our results show that the reduction of climate change impact through the employment of green H_2 transport routes shifts environmental burdens to other impact categories.

3.2.3. *Sensitivity analysis of the Global Warming Impact of the electricity source and transport distance*

In this section, the GWI of electricity supply as well as the transport distance are varied within a sensitivity analysis. In Fig. 9, the GWI of H_2 transport routes are shown in dependence of the GWI of electricity supply. The fossil benchmark is basically independent from electricity supply and thus shows an almost horizontal line. In contrast, the green

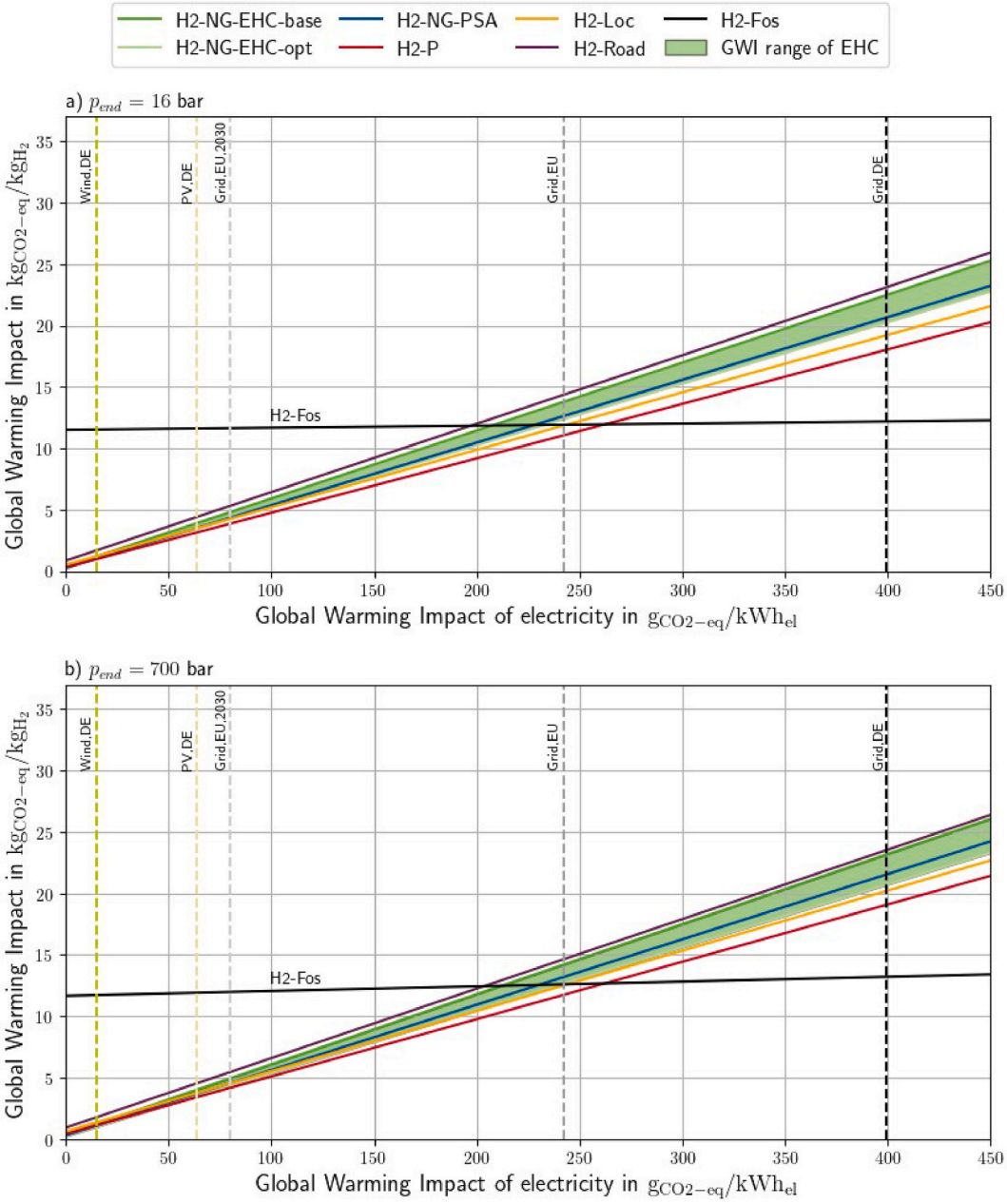

Fig. 9. Sensitivity analysis of the total Global Warming Impact (GWI) with respect to the GWI for the electricity source used in the H_2 supply chain for 20 vol.-% H_2 and p_{sec} = 16 bar. The transport distance is 1000 km. We assume that the fraction of the existing pipeline capacity used to transport H_2 during H_2/NG co-transport was previously unused and available as excess capacity (see Table 1). H_2-NG-EHC-base and H_2-NG-EHC-opt are transport routes where H_2 is co-transported with natural gas (NG) and then separated via Electrochemical Hydrogen Compression (EHC). Base and opt refer to the base and optimistic case of the EHC. In H_2-NG-PSA, H_2 is co-transported with NG but subsequently separated via a Pressure Swing Adsorption (PSA). H_2–P describes H_2 transport in pure H_2 pipelines, H_2-Loc describes the transport of electricity with subsequent decentral H_2 production at the consumer-site and H_2-Road describes the transport of liquid H_2 in fuel-cell electricic trucks. H_2-Fos is the fossil benchmark where H_2 is produced via Steam Methane Reforming (SMR) and transported via H_2 pipelines. p_{end}: Final pressure of the H_2 product, p_{sec} : Operating pressure of the secondary pipeline (see Fig. 1). DE: Germany, EU: Europe.

H_2 transport routes depend heavily on the GWI of electricity supply: the steep slopes of the green H_2 transport routes indicate that due to a large electricity demand within the supply chain, the GWI of electricity supply dominates the overall GWI of H_2 supply. Differences among the green H_2 transport options have a much smaller effect. The overall GWI of the green H_2 transport routes can even exceed that of fossil H_2. For example, powering the supply chain with German grid electricity would lead to GWI more than twice as high as fossil H_2. For most of the transport routes, even the GWI of the current European grid mix would not be sufficient to achieve a lower GWI than fossil H_2. However, increasing the share of renewable energy sources leads to a lower GWI than fossil H_2. For example, using the 2030 European grid mix (80 $g_{CO2\text{-}eq}/kwh_{el}$) results in more than 50 % reduction in GWI compared to fossil H_2 for all green H_2 transport routes. The usage of PV- or wind-electricity leads to an even higher reduction. Therefore, we emphasize that it is essential to power the entire H_2 supply chain with as much renewable electricity as possible.

Fig. S9 in SI shows a zoomed-in view of Fig. 9, which highlights that H_2/NG co-transport with EHC-opt or PSA can achieve a lower GWI than pure H_2 pipelines for both end pressure cases. H_2/NG co-transport with EHC-opt has a lower GWI than with PSA, while H_2/NG co-transport with EHC-base has a higher GWI than with PSA for both end pressure cases and regardless of the GWI for electricity in the supply chain.

The influence of the transport distance is shown in Fig. 10, together with a variation of the GWI of electricity. In a heat map, the most favorable transport route is identified for each combination of transport distance and GWI of electricity supply. With respect to both parameters, pure H_2 pipelines and H_2/NG co-transport with EHC-opt achieve the lowest GWI as they cover the largest areas in Fig. 10. In accordance to the results in Fig. 9, as long as the electricity has a GWI above ~260 $g_{CO2\text{-}eq}/kwh_{el}$, fossil H_2 has a lower GWI than all green H_2 transport routes.

As Fig. 10 shows, the area where H_2/NG co-transport with EHC-opt is preferred increases with rising transport distances and for p_{end} = 700 bar. The shift in the preferred transport route with increasing transport distance is driven by the growing difference in transport impacts between pure H_2 pipelines and H_2/NG co-transport with EHC-opt (compare Section 3.2.1). For p_{end} = 700 bar, pure H_2 pipelines require an additional compression of the H_2 product, which is not required for p_{end} = 16 bar as the pipeline operating pressure is 16 bar. Therefore, for

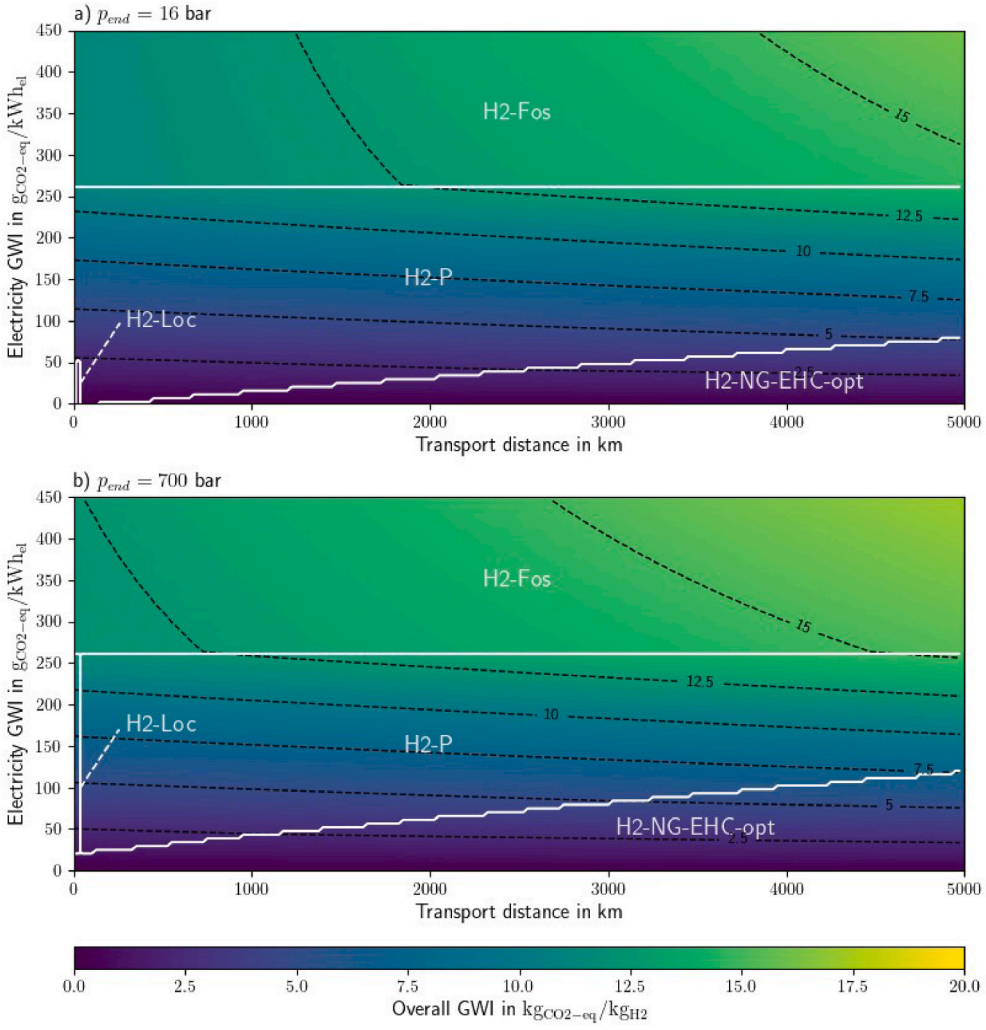

Fig. 10. Heat map depicting the most favorable transport route and its overall Global Warming Impact (GWI) with respect to the transport distance and the GWI for the electricity source used in the hydrogen supply chain for 20 vol.-% hydrogen and p_{sec} = 16 bar. We assume that the fraction of the existing pipeline capacity used to transport H_2 during H_2/NG co-transport was previously unused and available as excess capacity (see Table 1). p_{end}: Final pressure of the H_2 product, p_{sec} : Operating pressure of the secondary pipeline (see Fig. 1). H_2-NG-EHC-opt are transport routes where hydrogen is co-transported with natural gas (NG) and then separated via Electrochemical Hydrogen Compression (EHC). Base and opt refer to the base and optimistic case of the EHC. H_2–P describes hydrogen transport in pure hydrogen pipelines, H_2-Loc describes the transport of electricity with subsequent decentral hydrogen production at the consumer-site. H_2-Fos is the fossil benchmark where hydrogen is produced via Steam Methane Reforming (SMR) and transported via hydrogen pipelines. p_{end}: Final pressure of the hydrogen product.

p_{end} = 16 bar, the lower transport impacts for H_2/NG co-transport with EHC-opt need to offset the additional impacts associated with separation and compression.

Figs. S15–S24 in Section 3.3 of the SI includes the heatmap in Fig. 10 for all the other cases (see Table 1). For electricity with low GWI and long transport distances, H_2/NG co-transport with EHC-opt is the optimal transport route in every considered case. If the unrecovered H_2/NG mixture of the PSA can be fed into a pipeline operating at desorption pressure of 1 bar (p_{sec} = 1 bar), H_2/NG co-transport with PSA can also achieve the lowest GWI. If the fraction of the existing pipeline capacity used to transport H_2 during H_2/NG co-transport was previously used to transport NG (no excess capacity), the preferred area for pure H_2 pipelines increases as the transport impacts for the H_2/NG co-transport routes increase.

The sensitivity analyses allow us to make robust conclusions across all considered parameter variations: First, all green H_2 transport routes achieve lower GWI than fossil H_2 production if the GWI of electricity remains below the ~260 $g_{CO2\text{-}eq}/kwh_{el}$ threshold identified in Fig. 9, and second, H_2/NG co-transport with EHC consistently has a lower GWI than liquid H_2 transport via trucks, regardless of the considered EHC model and electricity GWI. However, the ranking between H_2/NG co-transport with EHC, PSA and pure H_2 pipelines is conditional and depends on the transport distance, end pressure, secondary pipeline pressure and the EHC model. The range between the base and optimistic EHC models can thus be interpreted as the uncertainty range in EHC performance at this stage of development.

In summary, H_2/NG co-transport with subsequent separation and compression via EHC has the potential to achieve similar or lower GWI as H_2 pipelines and H_2/NG co-transport with PSA, especially for long transport distances and high compression ratios, provided that the assumptions of the optimistic model need to be met.

3.3. Discussion

Our work assesses the environmental potential of Electrochemical Hydrogen Compression (EHC). We develop a base and optimistic model of EHC based on a 1D simulation model with several simplifications: The feed gas is assumed to consist of methane and H_2, neglecting other components within NG that could affect the performance of the EHC. In the optimistic case, we use literature data to model a membrane with higher conductivity leading to lower ohmic resistances. We further assume a faradaic efficiency of 100 %, which implies that neither H_2 back-diffusion losses nor incomplete reactions occur, even for high compression ratios. This assumption is rather optimistic and we emphasize that further research is needed to reach these conditions. In contrast, the base model accounts for these losses and represents current EHC performance, such that both models capture the uncertainty range in EHC efficiency. Nonetheless, EHC is already commercially available and high compression ratios have been shown to be reachable. For example, the Dutch startup HyET managed to develop an EHC stack, which can achieve H_2 pressures up to 900 bar in a single-stage compression [22].

Most important, our environmental assessment highlights that it is essential to power the green H_2 routes with renewable electricity. For most countries, using grid electricity with the current environmental impacts leads to a GWI higher than that of fossil H_2 production. This is especially relevant for H_2/NG co-transport with EHC since the subsequent electrochemical separation and compression causes additional energy demands compared to the other H_2 transport routes. Consequently, the environmental performance of EHC is particularly sensitive to the GWI of electricity supply, and the favorable results in this study rely on the use of electricity with low GWI.

While the considered green H_2 transport routes reduce the greenhouse gas (GHG) emissions compared to fossil H_2 production, the GHG emission reductions are accompanied by increased impacts in 9-11 out of 16 environmental categories. Consequently, there is an environmental burden-shift. Further investigation is required to assess the severity of the environmental burden-shift, e.g., by performing an absolute environmental sustainability assessment [75]. Although we assume wind electricity as the electricity source, the environmental burden associated with electricity use are significant due to the material demands in the wind power supply chain. For EHC specifically, the increased electricity demand as well as the material demands for the membrane and catalyst contribute to increased impacts in several categories. Besides reducing the overall electricity demand of EHC through improved energetic efficiency, the development of novel membrane materials with higher conductivity and reduced use of precious metal catalysts such as platinum are needed to reduce the environmental impacts. Improved material circularity through recycling and circular design of electrochemical components can further reduce environmental burden. Future work should include a prospective LCA of the material supply chain to account for expected changes in material production.

Our work shows that the integration of EHC into high-pressure NG distribution pipelines enables H_2 supply to H_2 consumers with low GHG emissions. Besides EHC, we consider PSA as separation unit in NG pipelines. The environmental impacts of PSA depend on which NG pipelines are available near the H_2 consumer. If the H_2 consumer is only connected to high-pressure distribution pipelines, additional energy for the PSA setup is needed to compress the unrecovered H_2/NG mixture. This energy demand increases for low volume percentages of H_2, since the amount of NG in the unrecovered H_2/NG mixture increases. In that case, PSA has higher environmental impacts than the optimistic model of EHC, and at 5 vol.-% H_2 even higher than those of the base model of EHC. If the consumer is connected to low- or mid pressure distribution pipelines, the integration of PSA leads to similar environmental impacts as the optimistic model of the EHC. Therefore, the comparison of EHC with PSA shows that EHC can achieve lower environmental impacts than PSA in most cases and offers higher design flexibility. Thus, if future development targets of the optimistic EHC model are met, it can enable H_2 supply via existing NG pipelines with lower environmental impacts than PSA. However, further assessment regarding economic feasibility and technical scale-up considerations is needed to fully evaluate whether EHC is more suitable for large-scale deployment.

According to the German association for gas and water (DVGW), German gas grids are ready to transport up to 20 vol.-% of H_2 [37]. If renewable electricity powers the entire supply chain, the co-transport of 20 vol.-% H_2 with subsequent separation and compression via EHC can lead to a lower GWI than transport in H_2 pipelines, especially for long transport distances and high compression ratios. Compared to the fossil H_2 production, all considered green H_2 transport routes can achieve a GWI reduction of at least 84 %, while H_2/NG co-transport with 20 vol.-% H_2 and subsequent separation and compression via the optimistic model of EHC can achieve a GWI reduction of up to 91 % if wind electricity is used to power the entire supply chain. Accordingly, H_2/NG co-transport is a promising H_2 transport option but should be regarded as complementary and not a substitute to pure H_2 pipelines. In particular, H_2/NG co-transport could serve as an interim solution to supply H_2 consumers that are not yet connected to a dedicated H_2 pipeline network. Within H_2/NG co-transport, EHC has the potential to be an essential technology for the distribution of high-purity and compressed H_2 using existing NG infrastructure, provided that future development targets are met.

4. Conclusions

We conducted a cradle-to-gate LCA to compare the environmental impacts of hydrogen (H_2) and natural gas (NG) co-transport in existing NG pipelines with subsequent separation and compression via EHC to other green H_2 transport options in 16 environmental impact categories. To capture the uncertainty range of EHC, we developed a base and optimistic case of EHC.

H_2/NG co-transport in existing NG pipelines with subsequent separation and compression via EHC has the potential to achieve lower

environmental impacts than transport via H_2 pipelines, especially for high H_2 end pressures and long transport distances. By relying on existing infrastructure, environmental impacts of H_2 transport can be reduced during H_2/NG co-transport. The optimistic EHC model has the potential to also achieve lower environmental impacts than Pressure Swing Adsorption (PSA), while the base model has a higher GWI than PSA, highlighting the importance of EHC efficiency improvements. All considered green H_2 transport routes can achieve greenhouse gas (GHG) emission reductions of at least 84 % compared to the fossil production, while H_2/NG co-transport with 20 vol.-% H_2 with EHC can reach GHG emission reductions of up to 91 % if wind power is used to power the supply chain. The GHG emissions of the electricity powering the supply chain is the dominant driver of the overall GHG emissions of green H_2 supply. If the GWI of the electricity exceeds ~260 $g_{CO2\text{-}eq}/kWh_{el}$, the GHG emissions of green H_2 supply options can even exceed those of fossil H_2. The deployment of green H_2 transport routes causes environmental burden-shift in at least 9 impact categories.

H_2/NG co-transport represents a promising complementary option to new pure H_2 pipelines. In particular, H_2/NG co-transport can be utilized to supply H_2 consumers in regions where NG infrastructure is available but no dedicated H_2 pipeline exists. EHC is a promising technology for large-scale H_2 distribution, as EHC enables the use of the extensive NG infrastructure for high-purity H_2 supply with low GHG emissions. However, efficiency improvements through novel membrane and catalyst materials for EHC are necessary to reach the environmental performance of the optimistic model in this work. Future work should also focus on investigating environmental burden-shift through absolute sustainability assessments and advancements of EHC by researching novel membrane and catalyst materials to improve efficiency and material circularity. As economic feasibility of EHC will ultimately drive its adoption, future work should integrate our environmental assessment with a techno-economic analysis.

CRediT authorship contribution statement

Karan Anand: Writing – original draft, Visualization, Validation, Software, Methodology, Investigation, Data curation, Conceptualization. **Georgia Ioanna Prokopou:** Writing – review & editing, Conceptualization. **Wibke Zängler:** Writing – review & editing, Project administration, Conceptualization. **Vu Phong Nguyen:** Writing – review & editing, Software, Investigation, Data curation. **Hendrik Pötting:** Writing – review & editing, Visualization, Supervision, Methodology, Conceptualization. **Robert Keller:** Supervision, Project administration, Funding acquisition. **Alexander Mitsos:** Writing – review & editing, Supervision, Funding acquisition. **Matthias Wessling:** Supervision, Project administration, Funding acquisition. **Niklas von der Assen:** Writing – review & editing, Visualization, Supervision, Methodology, Funding acquisition, Conceptualization.

Declaration of competing interest

The authors declare that they have no known competing financial interests or personal relationships that could have appeared to influence the work reported in this paper.

Acknowledgments

This work was funded by the German Federal Ministry for Education and Research (BMBF) within the project HyInnoSep of Zukunftscluster Wasserstoff (grant number 03ZU1115CA). Support from the Deutsche Forschungsgemeinschaft (DFG) within the project IRTG 2983 Hy-Potential (ID: 516338899) is gratefully acknowledged.

Appendix A. Supplementary data

Supplementary data to this article can be found online at https://doi.org/10.1016/j.ijhydene.2026.154957.

Abbreviations

RES	Renewable electricity sources
H_2	Hydrogen
NG	Natural gas
PSA	Pressure Swing Adsorption
EHC	Electrochemical Hydrogen Compression
SMR	Steam Methane Reforming
GHG	Greenhouse gas
GWI	Global Warming Impact
JRC	Joint Research Center of the European Commission
LCA	Life Cycle Assessment
FU	Functional Unit
H_2-NG-EHC-base	Hydrogen and natural gas co-transport with subsequent separation and compression via base model of EHC
H_2-NG-EHC-opt	Hydrogen and natural gas co-transport with subsequent separation and compression via optimistic model of EHC
H_2-NG-PSA	Hydrogen and natural gas co-transport with subsequent separation and compression via PSA
H_2–P	Hydrogen transport in pure hydrogen pipelines
H_2-Road	Transport of liquid hydrogen in fuel-cell electricic trucks
H_2-Loc	Transport of electricity with subsequent decentral hydrogen production at the consumer-site
H_2-Fos	Fossil benchmark where hydrogen is produced via Steam Methane Reforming (SMR) and transported via hydrogen pipelines
p_{end}	Final pressure of the hydrogen product
p_{op}	Operating pressure of the primary pipeline
p_{sec}	Operating pressure of the secondary pipeline
PEM	Proton exchange membrane
LCI	Life Cycle Inventory
LCIA	Life Cycle Impact Assessment
HVAC	High-voltage alternating current
EF	Environmental footprint

Mathematical symbols

x_{H2}	Molar fraction of hydrogen in the H_2/NG mixture
$w_{tot,EHC}$	Total energy demand of EHC
$w_{el,EHC}$	Electric energy demand of EHC
$w_{th,EHC}$	Heating demand of EHC
$w_{cool,EHC}$	Cooling demand of EHC
$m_{NG,not-Co}$	NG mass transported in the fraction of the pipeline capacity used to transport H_2 in the H_2/NG co-transported pipeline
$m_{NG,Co}$	NG mass transported with H_2 in the H_2/NG co-transported pipeline
$m_{H2,Co}$	H_2 mass transported during H_2/NG co-transport

References

[1] Schreyer F, Ueckerdt F, Pietzcker R, Rodrigues R, Rottoli M, Madeddu S, Pehl M, Hasse R, Luderer G. Distinct roles of direct and indirect electrification in pathways to a renewables-dominated European energy system. One Earth 2024;7:226–41. https://doi.org/10.1016/j.oneear.2024.01.015.

[2] Evro S, Oni BA, Tomomewo OS. Carbon neutrality and hydrogen energy systems. Int J Hydrogen Energy 2024;78:1449–67. https://doi.org/10.1016/j.ijhydene.2024.06.407.

[3] Abdin Z, Zafaranloo A, Rafiee A, Mérida W, Lipiński W, Khalilpour KR. Hydrogen as an energy vector. Renew Sustain Energy Rev 2020;120. https://doi.org/10.1016/j.rser.2019.109620.

[4] Mio A, Barbera E, Massi Pavan A, Bertucco A, Fermeglia M. Sustainability analysis of hydrogen production processes. Int J Hydrogen Energy 2024;54:540–53. https://doi.org/10.1016/j.ijhydene.2023.06.122.

[5] Fuel cells and hydrogen 2 joint undertaking, Hydrogen roadmap Europe - a sustainable pathway for the European energy transition. 2019. https://doi.org/10.2843/249013.

[6] Korberg AD, Thellufsen JZ, Skov IR, Chang M, Paardekooper S, Lund H, Mathiesen BV. On the feasibility of direct hydrogen utilisation in a fossil-free Europe. Int J Hydrogen Energy 2023;48:2877–91. https://doi.org/10.1016/j.ijhydene.2022.10.170.

[7] Akhtar MS, Dickson R, Liu JJ. Life cycle assessment of inland green hydrogen supply chain networks with current challenges and future prospects. ACS Sustainable Chem Eng 2021;9:17152–63. https://doi.org/10.1021/acssuschemeng.1c06769.

[8] Lipiäinen S, Lipiäinen K, Ahola A, Vakkilainen E. Use of existing gas infrastructure in European hydrogen economy. Int J Hydrogen Energy 2023;48:31317–29. https://doi.org/10.1016/j.ijhydene.2023.04.283.

[9] Die Nationale Wasserstoffstrategie. Bundesministerium für Wirtschaft und Energie (BMWi) 2020. https://www.bundeswirtschaftsministerium.de/Redaktion/DE/Publikationen/Energie/die-nationale-wasserstoffstrategie.pdf?_blob=publicationFile&v=11. [Accessed 18 September 2025].

[10] Bundesministerium für Wirtschaft und Klimaschutz (BMWK). Fortschreibung der Nationalen Wasserstoffstrategie NWS; 2023. 2023, https://www.bundeswirtschaftsministerium.de/Redaktion/DE/Publikationen/Energie/fortschreibung-nationale-wasserstoffstrategie.pdf?_blob=publicationFile&v=9. [Accessed 18 September 2025].

[11] Cristello JB, Yang JM, Hugo R, Lee Y, Park SS. Feasibility analysis of blending hydrogen into natural gas networks. Int J Hydrogen Energy 2023;48:17605–29. https://doi.org/10.1016/j.ijhydene.2023.01.156.

[12] Witkowski A, Rusin A, Majkut M, Stolecka K. Analysis of compression and transport of the methane/hydrogen mixture in existing natural gas pipelines. Int J Pres Ves Pip 2018;166:24–34. https://doi.org/10.1016/j.ijpvp.2018.08.002.

[13] Department of Climate Change. Energy, the environment and water, National hydrogen strategy Australia. Barrington Stoke; 2024.

[14] Zou J, Han N, Yan J, Feng Q, Wang Y, Zhao Z, Fan J, Zeng L, Li H, Wang H. Electrochemical compression technologies for high-pressure hydrogen: current status, challenges and perspective. Electrochem Energy Rev 2020;3:690–729. https://doi.org/10.1007/s41918-020-00077-0.

[15] Prokopou GI, Faust JMM, Mitsos A, Bongartz D. Cost-optimal design and operation of hydrogen refueling stations with mechanical and electrochemical hydrogen compressors. Comput Chem Eng 2025;192:108862. https://doi.org/10.1016/j.compchemeng.2024.108862.

[16] Dehdari L, Burgers I, Xiao P, Li K Gang, Singh R, Webley PA. Purification of hydrogen from natural gas/hydrogen pipeline mixtures. Sep Purif Technol 2022;282(Part B). https://doi.org/10.1016/j.seppur.2021.120094.

[17] Nordio M, Wassie SA, Van Sint Annaland M, Pacheco Tanaka DA, Viviente Sole JL, Gallucci F. Techno-economic evaluation on a hybrid technology for low hydrogen concentration separation and purification from natural gas grid. Int J Hydrogen Energy 2021;46:23417–35. https://doi.org/10.1016/j.ijhydene.2020.05.009.

[18] Rhandi M, Trégaro M, Druart F, Deseure J, Chatenet M. Electrochemical hydrogen compression and purification versus competing technologies: part I. Pros and cons. Chin J Catal 2020;41:756–69. https://doi.org/10.1016/S1872-2067(19)63404-2.

[19] Liemberger W, Groß M, Miltner M, Harasek M. Experimental analysis of membrane and pressure swing adsorption (PSA) for the hydrogen separation from natural gas. J Clean Prod 2017;167:896–907. https://doi.org/10.1016/j.jclepro.2017.08.012.

[20] Aykut Y, Yurtcan AB. The role of the EHC system in the transition to a sustainable energy future: a review. Int J Hydrogen Energy 2023;48:23089–109. https://doi.org/10.1016/j.ijhydene.2023.03.109.

[21] Prokopou GI, Mödden ML, Mitsos A, Bongartz D. Optimal sizing and operation of electrochemical hydrogen compression. Chem Eng Sci 2024;293. https://doi.org/10.1016/j.ces.2024.120031.

[22] HyET - efficient hydrogen purification & compression. https://hyethydrogen.com/compression/. [Accessed 23 April 2025].

[23] Marciuš D, Kovač A, Firak M. Electrochemical hydrogen compressor: recent progress and challenges. Int J Hydrogen Energy 2022;47:24179–93. https://doi.org/10.1016/j.ijhydene.2022.04.134.

[24] Neacsa A, Eparu CN, Stoica DB. Hydrogen–natural gas blending in distribution systems—an energy, economic, and environmental assessment. Energies 2022;15. https://doi.org/10.3390/en15176143.

[25] Cappello V, Sun P, Elgowainy A. Blending low-carbon hydrogen with natural gas: impact on energy and life cycle emissions in natural gas pipelines. Gas Sci Eng 2024;128. https://doi.org/10.1016/j.jgsce.2024.205389.

[26] Di Lullo G, Oni AO, Kumar A. Blending blue hydrogen with natural gas for direct consumption: examining the effect of hydrogen concentration on transportation and well-to-combustion greenhouse gas emissions. Int J Hydrogen Energy 2021;46:19202–16. https://doi.org/10.1016/j.ijhydene.2021.03.062.

[27] Davis M, Okunlola A, Di Lullo G, Giwa T, Kumar A. Greenhouse gas reduction potential and cost-effectiveness of economy-wide hydrogen-natural gas blending for energy end uses. Renew Sustain Energy Rev 2023;171. https://doi.org/10.1016/j.rser.2022.112962.

[28] Bellocchi S, De Falco M, Facchino M, Manno M. Hydrogen blending in Italian natural gas grid: scenario analysis and LCA. J Clean Prod 2023;416. https://doi.org/10.1016/j.jclepro.2023.137809.

[29] Aminov RZ, Bairamov AN, Filippov SP. Comprehensive assessment of the effectiveness of the hydrogen production and transportation system. Int J Hydrogen Energy 2024;86:1358–75. https://doi.org/10.1016/j.ijhydene.2024.08.357.

[30] Di Lullo G, Giwa T, Okunlola A, Davis M, Mehedi T, Oni AO, Kumar A. Large-scale long-distance land-based hydrogen transportation systems: a comparative techno-economic and greenhouse gas emission assessment. Int J Hydrogen Energy 2022;47:35293–319. https://doi.org/10.1016/j.ijhydene.2022.08.131.

[31] Fazio S, Biganzioli F, De Laurentiis V, Zampori L, Sala S, Diaconu E. Supporting information to the characterisation factors of recommended EF Life Cycle Impact Assessment methods. European Commission; 2018. https://doi.org/10.2760/002447.

[32] DIN Deutsches Institut für Normung e. V.. Umweltmanagement – Ökobilanz – Grundsätze und Rahmenbedingungen (ISO 14040:2006 + Amd 1:2020). Deutsche Fassung EN ISO 14040:2006 + A1:2020. Berlin: Beuth Verlag GmbH; 2021.

[33] Barthélémy H. Hydrogen storage - industrial prospectives. Int J Hydrogen Energy 2012;37:17364–72. https://doi.org/10.1016/j.ijhydene.2012.04.121.

[34] Al-Sharafi A, Al-Buraiki AS, Al-Sulaiman F, Antar MA. Hydrogen refueling stations powered by hybrid PV/wind renewable energy systems: Techno-socio-economic assessment. Energy Convers Manag X 2024;22. https://doi.org/10.1016/j.ecmx.2024.100584.

[35] International Organization for Standardization (ISO). ISO 14687:2019-11 Beschaffenheit von Wasserstoff als Kraftstoff - spezifizierung des Produkts. 2019.

[36] Hertwich EG, Gibon T, Bouman EA, Arvesen A, Suh S, Heath GA, Bergesen JD, Ramirez A, Vega MI, Shi L. Integrated life-cycle assessment of electricity-supply scenarios confirms global environmental benefit of low-carbon technologies. Proc Natl Acad Sci USA 2015;112:6277–82. https://doi.org/10.1073/pnas.1312753111.

[37] Deutscher Verein des Gas- und Wasserfachs e.V. (DVGW). Größtenteils bereits H2-ready: Netze, Speicher, Komponenten. 2023. https://www.dvgw.de/medien/dvgw/leistungen/publikationen/groesstenteils-h2ready-dvgw.pdf. [Accessed 19 July 2025].

[38] Wernet G, Bauer C, Steubing B, Reinhard J, Moreno-Ruiz E, Weidema B. The ecoinvent database version 3 (part I): overview and methodology. Int J Life Cycle Assess 2016;21:1218–30. https://doi.org/10.1007/s11367-016-1087-8.

[39] de Kleijne K, Huijbregts MAJ, Knobloch F, van Zelm R, Hilbers JP, de Coninck H, Hanssen SV. Worldwide greenhouse gas emissions of green hydrogen production and transport. Nat Energy 2024. https://doi.org/10.1038/s41560-024-01563-1.

[40] Bareiß K, de la Rua C, Möckl M, Hamacher T. Life cycle assessment of hydrogen from proton exchange membrane water electrolysis in future energy systems. Appl Energy 2019;237:862–72. https://doi.org/10.1016/j.apenergy.2019.01.001.

[41] Sharma H, Mandil G, Zwolinski P, Cor E, Mugnier H, Monnier E. Integration of life cycle assessment with energy simulation software for polymer exchange membrane (PEM) electrolysis. Proced CIRP 2020:176–81. https://doi.org/10.1016/j.procir.2020.02.139. Elsevier B.V.

[42] Mehmeti A, Angelis-Dimakis A, Arampatzis G, McPhail SJ, Ulgiati S. Life cycle assessment and water footprint of hydrogen production methods: from conventional to emerging technologies. Environments - MDPI 2018;5:1–19. https://doi.org/10.3390/environments5020024.
[43] Antonini C, Treyer K, Streb A, van der Spek M, Bauer C, Mazzotti M. Hydrogen production from natural gas and biomethane with carbon capture and storage - a techno-environmental analysis. Sustain Energy Fuels 2020;4:2967–86. https://doi.org/10.1039/d0se00222d.
[44] Yin L, Ju Y. Review on the design and optimization of hydrogen liquefaction processes. Front Energy 2020;14:530–44. https://doi.org/10.1007/s11708-019-0657-4.
[45] Al Ghafri SZ, Munro S, Cardella U, Funke T, Notardonato W, Trusler JPM, Leachman J, Span R, Kamiya S, Pearce G, Swanger A, Rodriguez ED, Bajada P, Jiao F, Peng K, Siahvashi A, Johns ML, May EF. Hydrogen liquefaction: a review of the fundamental physics, engineering practice and future opportunities. Energy Environ Sci 2022;15:2690–731. https://doi.org/10.1039/d2ee00099g.
[46] Peschel A. Industrial perspective on hydrogen purification, compression, storage, and distribution. Fuel Cells 2020;20:385–93. https://doi.org/10.1002/fuce.201900235.
[47] Stolzenburg K, Mubbala R. Integrated design for demonstration of efficient liquefaction of hydrogen (IDEALHY) - hydrogen liquefaction report. 2013.
[48] Kanz O, Brüggemann F, Ding K, Bittkau K, Rau U, Reinders A. Life-cycle global warming impact of hydrogen transport through pipelines from Africa to Germany. Sustain Energy Fuels 2023;7:3014–24. https://doi.org/10.1039/d3se00281k.
[49] Tahan MR. Recent advances in hydrogen compressors for use in large-scale renewable energy integration. Int J Hydrogen Energy 2022;47:35275–92. https://doi.org/10.1016/j.ijhydene.2022.08.128.
[50] Khan MA, Young C, Mackinnon C, Layzell DB. The techno-economics of hydrogen compression. Transition Accelerator Technical Briefs 2021;1:1–36.
[51] Cebolla O, Dolci R, Dolci F. Assessment of hydrogen delivery options. Luxembourg: Publications Office of the European Union; 2022. https://doi.org/10.2760/869085.
[52] European Comission JRC, Arrigoni A, Dolci F, Ortiz Cebolla R, Weidner E, D'Agostini T, Eynard U, Santucci V, Mathieux F. Environmental life cycle assessment (LCA) comparison of hydrogen delivery options within Europe. Luxembourg: Publications Office of the European Union; 2024. https://doi.org/10.2760/5459.
[53] Télessy K, Barner L, Holz F. Repurposing natural gas pipelines for hydrogen: limits and options from a case study in Germany. Int J Hydrogen Energy 2024;80:821–31. https://doi.org/10.1016/j.ijhydene.2024.07.110.
[54] Rödl A, Wulf C, Kaltschmitt M. Assessment of selected hydrogen supply chains-factors determining the overall GHG emissions. Hydrogen Supply Chain: Design, Deployment and Operation 2018:81–109. https://doi.org/10.1016/B978-0-12-811197-0.00003-8. Elsevier.
[55] Wulf C, Reuß M, Grube T, Zapp P, Robinius M, Hake JF, Stolten D. Life Cycle Assessment of hydrogen transport and distribution options. J Clean Prod 2018;199:431–43. https://doi.org/10.1016/j.jclepro.2018.07.180.
[56] Direct current for long-distance transmission. https://medienportal.siemens-stiftung.org/de/direct-current-for-long-distance-transmission-101614. [Accessed 16 January 2025].
[57] Sacchi R, Bauer C, Cox BL. Does size matter? The influence of size, load factor, range autonomy, and application type on the life cycle assessment of current and future medium? The heavy-duty vehicles. Environ Sci Technol 2021;55:5224–35. https://doi.org/10.1021/acs.est.0c07773.
[58] Weiszflog E, Abbas M. Life cycle assessment of hydrogen storage systems for trucks. Chalmers University of Technology; 2022.
[59] Laouir A. Performance analysis of open-loop cycles for LH2 regasification. Int J Hydrogen Energy 2019;44:22425–36. https://doi.org/10.1016/j.ijhydene.2018.12.204.
[60] Mrusek S, Blasius M, Morgenroth F, Thiele S, Wasserscheid P. Hydrogen extraction from methane-hydrogen mixtures from the natural gas grid by means of electrochemical hydrogen separation and compression. Int J Hydrogen Energy 2024;50:526–38. https://doi.org/10.1016/j.ijhydene.2023.08.195.
[61] Abdulla A, Laney K, Padilla M, Sundaresan S, Benziger J. Efficiency of hydrogen recovery from reformate with a polymer electrolyte hydrogen pump. AIChE J 2011;57:1767–79. https://doi.org/10.1002/aic.12406.
[62] Yang J, Lee C-H, Chang J-W. Separation of hydrogen mixtures by a two-bed pressure swing adsorption process using zeolite 5A. Ind Eng Chem Res 1997. https://doi.org/10.1021/ie960728h.
[63] Burgers I, Dehdari L, Xiao P, Li K Gang, Goetheer E, Webley P. Techno-economic analysis of PSA separation for hydrogen/natural gas mixtures at hydrogen refuelling stations. Int J Hydrogen Energy 2022;47:36163–74. https://doi.org/10.1016/j.ijhydene.2022.08.175.
[64] Shabbani HJK, Othman MR, Al-Janabi S, Barron A, Helwani Z. H2 purification employing pressure swing adsorption process: parametric and bibliometric review. Int J Hydrogen Energy 2024;50:674–99. https://doi.org/10.1016/j.ijhydene.2023.11.069.
[65] Sircar S, Golden TC. Purification of hydrogen by pressure swing adsorption. Separ Sci Technol 2000;35:667–87. https://doi.org/10.1081/SS-100100183.
[66] Sand M, Skeie RB, Sandstad M, Krishnan S, Myhre G, Bryant H, Derwent R, Hauglustaine D, Paulot F, Prather M, Stevenson D. A multi-model assessment of the Global Warming Potential of hydrogen. Commun Earth Environ 2023;4. https://doi.org/10.1038/s43247-023-00857-8.
[67] Derwent RG, Stevenson DS, Utembe SR, Jenkin ME, Khan AH, Shallcross DE. Global modelling studies of hydrogen and its isotopomers using STOCHEM-CRI: likely radiative forcing consequences of a future hydrogen economy. Int J Hydrogen Energy 2020;45:9211–21. https://doi.org/10.1016/j.ijhydene.2020.01.125.
[68] Hauglustaine D, Paulot F, Collins W, Derwent R, Sand M, Boucher O. Climate benefit of a future hydrogen economy. Commun Earth Environ 2022;3. https://doi.org/10.1038/s43247-022-00626-z.
[69] Warwick NJ, Archibald AT, Griffiths PT, Keeble J, O'connor FM, Pyle JA, Shine KP. Atmospheric composition and climate impacts of a future hydrogen economy. Atmos Chem Phys 2023;23:13451–67. https://doi.org/10.5194/acp-23-13451-2023.
[70] Lipp L. Electrochemical hydrogen compressor. https://www.hydrogen.energy.gov/docs/hydrogenprogramlibraries/pdfs/review14/pd048_lipp_2014_o.pdf. [Accessed 4 March 2026].
[71] Jackson C, Smith G, Kucernak AR. Deblending and purification of hydrogen from natural gas mixtures using the electrochemical hydrogen pump. Int J Hydrogen Energy 2024;52:816–26. https://doi.org/10.1016/j.ijhydene.2023.05.065.
[72] Nordio M, Rizzi F, Manzolini G, Mulder M, Raymakers L, Van Sint Annaland M, Gallucci F. Experimental and modelling study of an electrochemical hydrogen compressor. Chem Eng J 2019;369:432–42. https://doi.org/10.1016/j.cej.2019.03.106.
[73] V Dale N. Characterization of PEM electrolyzer and PEM fuel cell stacks characterization of PEM electrolyzer and PEM fuel cell stacks using electrochemical impedance spectroscopy using electrochemical impedance spectroscopy. https://commons.und.edu/theses; 2009.
[74] Department of Energy U. Hydrogen fuel R&D: U.S. department of energy hydrogen and fuel cells program 2019 Annual Merit Review (AMR) and peer evaluation report. 2019.
[75] Bjorn A, Paulilo A, Sanye Mengual E, De Laurentiis V, Vea E, Hauschild MZ, Sala S. Guidance for applying absolute environmental sustainability assessment on activities at different scales (BETA version). https://doi.org/10.2760/7677803; 2025.